GRAS SAF Report 12
Ref: SAF/GRAS/DMI/REP/GSR/012
Web: www.grassaf.org
Date: February 2, 2012

The EUMETSAT Network of Satellite Application Facilities

GRAS SAF
GRAS Meteorology

GRAS SAF Report 12

Assimilation of Global Positioning System Radio Occultation Data in the ECMWF ERA-Interim Re-analysis

P. Poli, S. B. Healy, and D. P. Dee

ECMWF

Document Author Table

	Name	Function	Date	Comments
Prepared by:	Paul Poli	ERA Interim	February 2, 2012	
Reviewed by:	Dick Dee	Satellite Section, ECMWF	October 5, 2009	
Approved by:	Kent Lauritsen	GRAS SAF Project Manager	February 25, 2010	

Document Change Record

Issue/Revision	Date	By	Description
Version 1.0	June 2009	SBH	For internal review
Version 1.1	February 25 2010	SBH	First Release
Version 1.2	February 2 2012	SBH	Web version pointing to QJ paper

GRAS SAF Project

The GRAS SAF is a EUMETSAT-funded project responsible for operational processing of GRAS radio occultation data from the Metop satellites. The GRAS SAF delivers bending angle, refractivity, temperature, pressure, and humidity profiles in near-real time and offline for NWP and climate users. The offline profiles are further processed into climate products consisting of gridded monthly zonal means of bending angle, refractivity, temperature, humidity, and geopotential heights together with error descriptions.

The GRAS SAF also maintains the Radio Occultation Processing Package (ROPP) which contains software modules that will aid users wishing to process, quality-control and assimilate radio occultation data from any radio occultation mission into NWP and other models.

The GRAS SAF Leading Entity is the Danish Meteorological Institute (DMI), with Cooperating Entities: i) European Centre for Medium-Range Weather Forecasts (ECMWF) in Reading, United Kingdom, ii) Institut D'Estudis Espacials de Catalunya (IEEC) in Barcelona, Spain, and iii) Met Office in Exeter, United Kingdom. To get access to our products or to read more about the project please go to http://www.grassaf.org.

1 Introduction

An updated verision of this report has been published (Poli, P., Healy, S. B. and Dee, D. P. (2010), Assimilation of Global Positioning System radio occultation data in the ECMWF ERA Interim reanalysis, Quarterly Journal of the Royal Meteorological Society, 136: 1972–1990. doi: 10.1002/qj.722).

Observing the Earth's atmosphere with the Global Positioning System (GPS) Radio Occultation (RO) technique was first demonstrated in 1995 with the GPS-Meteorology (GPS/MET) experiment (Kursinski et al., 1996; Ware et al., 1996). This observation technique monitors the refraction induced by the atmosphere on GPS radio waves (Kursinski et al., 1997) from a satellite on low-Earth orbit. The instrumentation is technically simple with no optics and no moving parts, but a GPS receiver and dedicated antennae oriented in the satellite roll direction. Because the atmospheric refraction in the neutral atmosphere (below the ionosphere) depends on pressure, temperature, and water vapor content, the assimilation of GPSRO measurements can be used to reduce errors in these variables in an analysis scheme (Kuo et al., 2000).

Several GPSRO experiments have followed the GPS/MET experiment, enabling upgrades in the instrument design and improvements in the data processing to be tested. The Global Navigation Satellite Systems Receiver for Atmospheric Sounding (GRAS instrument) is the first fully operational GPSRO mission, onboard the European Organisation for the Exploitation of Meteorological Satellites (Eumetsat) polar-orbiting operational satellite series (MetOp). The first satellite of that series (MetOp-A) was launched in 2006 and the series is expected to last until at least the year 2020, offering thus great prospects for a long GPSRO data record collected with a consistent instrument (Luntama et al., 2008).

Several studies have evaluated and proven the value of GPSRO for improving Numerical Weather Prediction (NWP) forecasts (Healy and Thépaut, 2006; Cucurull et al., 2007; Buontempo et al., 2008; Poli et al., 2008). In fact, GPSRO has quickly evolved from an experimental concept to become a mainstay of the observing system providing data assimilated without bias correction by several NWP national agencies worldwide.

During a GPSRO observation (occultation event), the observable of choice is a fraction or multiple of a GPS radio carrier wavelength. That wavelength also acts in the basic application of positioning, as the multiplication factor in the derivation of distances from measured pseudo-delays. For that reason, ensuring the stability of the GPS carrier wavelength is a cornerstone of the GPS design concept. To achieve such stability, the generation of GPS radio waves onboard the GPS satellites is synchronized with onboard atomic clocks; these highly stable clocks, to better than one part in 10^{12} (Logsdon, 1995) are themselves synchronized daily with atomic clocks on the ground. It has been argued that GPSRO measurements would inherit the atomic clock calibration feature, and are, as a result, stable over time (Goody et al., 1998). Current efforts are now aimed at using direct GPSRO measurements in climate studies, either to validate climate models (e.g., Leroy et al., 2006) or to derive climatologies and detect climate trends from the current record (e.g., Steiner et al., 2009) or in the future (e.g., Foelshe et al., 2007; Ringer and Healy, 2008).

In parallel to these GPSRO developments, great progress has been made on the issue of observation bias correction in data assimilation. Derber and Wu (1998) devised a method to correct the observation bias (resulting from measurement and representativeness systematic errors) in passive radiance brightness temperatures, using as references all the other observations available for the assimilation. This idea was recently applied at the European Centre for Medium-range Weather Forecasts (ECMWF), under the name of variational bias correction (VarBC: Dee, 2005; Auligné et al., 2007). In practice, VarBC in data assimilation enables to formally distinguish between observations that are considered stable and observations that need to be bias corrected (the bias correction of the latter being anchored to the former). Beyond the NWP application, and looking over long time periods, VarBC gives an opportunity to observations considered as climate-stable to be treated as such in data assimilation, while other observations can be bias corrected towards the stable observations.

The VarBC concept has been used in the recent ECMWF re-analysis, ERA-Interim, which extends from 1989 to the present time (Uppala et al., 2008; Dee and Uppala, 2009). As their names suggest, re-analyses analyse the weather observations with state-of-the-art data assimilation and numerical weather prediction systems. In ERA-Interim, the background created as the result of a previous analysis (projected in time by a prediction model) is compared every 12 hours against observations to create analysis increments. The products are global, gridded, multi-decadal time-series of meteorological analyses. Unlike the gridded products of daily operational numerical weather prediction, the products of a given re-analysis are free of discontinuities caused by model upgrades because a fixed configuration is used throughout the reanalysed time period. As a result, re-analyses reach users far beyond academic research (Hollingsworth and Pfrang, 2005).

The ERA-Interim re-analysis is not a replacement of the 45-year European global re-analysis (ERA-40, Uppala et al., 2005). Yet, it includes several improvements, such as a refined data assimilation scheme (four-dimensional variational assimilation, 4D-Var, with VarBC) and a refined numerical weather prediction model. Also, it is the first global re-analysis to assimilate GPSRO measurements. Data from the following three missions were assimilated in ERA-Interim: CHAllenging Mini-satellite Payload (CHAMP: Wickert et al., 2001), FORMOSAT-3/Constellation Observing System for Meteorology, Ionosphere and Climate (COSMIC: Anthes et al., 2008), and MetOp-A GRAS (Luntama et al., 2008).

Consequently, the assimilation of GPSRO data in the ERA-Interim 4D-Var with VarBC offers the first opportunities to study: the assimilation performance of GPSRO measurements in a long, multi-year experiment; the long-term comparison between GPSRO measurements and a data assimilation system with fixed characteristics (resolution, version); and the effect of GPSRO to act as a reference in the VarBC framework, where passive radiance observations are bias corrected.

This paper is organized as follows. Section 2 presents the ERA-Interim re-analysis system. Section 3 describes the GPSRO data and assimilation methodology. Section 4 reports on the actual use of GPSRO data. Section 5 compares GPSRO data with ERA-Interim background. Section 6 suggests possible impacts of GPSRO on the ERA-Interim re-analysis by looking at conjunctions between observed breaks in the time-series and the introduction of GPSRO data in large numbers. Section 7 assesses the validity of the suggested impacts, with the help of a data withholding experiment. A discussion of the results and open issues is included in section 8. Conclusions and perspectives for future work are given in section 9.

2 ERA-Interim Re-analysis System

Today's NWP models as run routinely by national agencies produce gridded representations of the atmosphere. These forecast products are based on analyses, which are updated several times per day using data collected world-wide and exchanged under the auspices of the World Meteorological Organization (WMO). The concept of re-analysis lies in the application of today's NWP and data assimilation techniques to past observations.

The first re-analyses were conducted to analyse the first global meteorological data collected for NWP, in 1979, during the First Global Global Atmospheric Research Program Experiment (FGGE: Bengtsson et al., 1982; Ploshay et al., 1992). The data collected at this occasion were reanalysed several times using various generations of NWP models. Although the original data had quickly lost their value for improving the operational forecast at the time, the successive re-analyses helped assess the improvement of NWP models in fitting the FGGE observations.

The latest ECMWF re-analysis, ERA-Interim, covers the satellite data-rich time period from 1989 to the present (Uppala et al., 2008). The production, started in 2006, has reached the real-time in the first quarter of 2009. Since then, the ERA-Interim archive is updated on a monthly basis, with a two- to three-month-delay. Of particular relevance for the current study, as compared to ERA-40, the ERA-Interim system features:

(i) an improved data assimilation scheme for the upper-air analyses, with a 12-hour 4D-Var instead of a 6-hour three-dimensional variational data assimilation (3D-Var);

(ii) a VarBC radiance correction scheme that is time adaptive, replacing the radiance bias correction that relied on piece-wise fixed predictors; that earlier approach had a tendency to introduce breaks in the ERA-40 products every time an additional passive sensor was introduced, or to prolong in time the effect of a model error if the predictors had been calculated during a time period with large model errors (for example after the Pinatubo eruption);

(iii) an improved analysis horizontal resolution (i.e., the resolution of the increments): spherical harmonics truncation T95 (approximately 210 km) in the first minimization and T159 (approximately 125 km) in the second minimization; and

(iv) an improved final product horizontal resolution, obtained from a forecast integration at horizontal resolution T255 (approximately 80 km).

The analysis and the forecast are discretized on 60 vertical levels between the surface and the 0.1 hPa pressure level. Further information about ERA-Interim product availability and characteristics can be found on the ECMWF re-analysis website (http://www.ecmwf.int/research/era).

The observations assimilated in ERA-Interim are mainly those prepared for ERA-40 between 1989 and 2002 (Uppala et al., 2005), and those received by ECMWF operations since 2002, with a few exceptions. The only additional datasets are reprocessed European Remote Sensing Satellite (ERS-1 and -2) altimeter wave heights, geostationary satellite winds reprocessed by Eumetsat, Global Ozone Monitoring Experiment (GOME) ozone data reprocessed

by the Rutherford Appleton Laboratory, and CHAMP GPSRO measurements reprocessed by the University Corporation for Atmospheric Research (UCAR).

3 GPSRO Data and Assimilation Methodology

Data from three GPSRO missions were assimilated in ERA-Interim. Table 3.1 shows the dates of data availability for each satellite, along with major gaps (defined as longer than 30 days).

The CHAMP satellite (Wickert et al., 2001) was launched in 2000. It is equipped with a Blackjack receiver instrument and collected data nearly continuously between May 2001 and 5 October 2008 (Jens Wickert, *personnal communication*). The mission is managed by the GeoForschungsZentrum (GFZ) in Postdam, Germany. The CHAMP data used here were reprocessed by the UCAR COSMIC Data Analysis and Archive Center (CDAAC).

The COSMIC constellation (Cheng et al., 2006), composed of six spacecraft (flight models 1–6, FM1–FM6), was launched in April 2006. Each spacecraft is fitted with an Integrated GPS Occultation Receiver (IGOR) instrument (Anthes et al., 2008). The mission has been collecting measurements since a few months after launch. The data used here were processed by the UCAR CDAAC for near-real-time provision to NWP centers.

The MetOp-A satellite, launched in October 2006, carries the GRAS instrument (Luntama et al., 2008). It has been collecting measurements nearly continuously since a few months after launch. The data used here were processed by Eumetsat for near-real-time provision to NWP centers.

Data from COSMIC and MetOp-A used in ERA-Interim are as received by ECMWF operations. Unlike the CHAMP reprocessed dataset, the COSMIC and MetOp-A GPSRO datasets were not obtained from reprocessing. The versions of processing softwares used by Eumetsat and UCAR CDAAC changed over time as the data providers upgraded their processing chains to incorporate new findings, mainly so as to improve the data yield (number of occultations) and quality. There is hence no guarantee that the quality of the COSMIC and MetOp-A data considered here is insensitive to changes in the data processing.

The GPSRO data assimilation methodology follows that originally developed by Healy and Thépaut (2006) for ECMWF NWP operations, with the assimilation of bending angle as a function of impact parameter. Throughout the text, when discussing results in bending angle space, we refer to impact height (Ao et al., 2003) as the vertical coordinate. The impact height is defined as the difference between the impact parameter and the local radius of curvature of the Earth. The difference between impact height h and altitude z for a given location depends on the actual atmospheric refractive index. That difference, always positive ($h > z$), decreases exponentially with increasing altitude, from about 2 km at the surface to less than 500 m above 10 km altitude.

The GPSRO observation errors are assumed to be unbiased and normally distributed in bending angle space. The observation error standard deviation, defined in percent of observation, decreases linearly with increasing impact height, from 20% at the surface to 1% at 10 km impact height, where it remains constant at 1% for higher impact heights greater than 10 km. There is a minimum observation error standard deviation of 6 μrad to reflect the effect of ionospheric noise in the stratosphere. The observation errors are also assumed

Table 3.1: GPSRO data assimilated in ERA-Interim between 1 January 1989 and 30 June 2009. Last column shows start and duration of gaps longer than 30 days

Satellite	Time period	Major gaps
CHAMP	May 2001 – May 2008	2 Nov 2004 (45 days) 2 Jul 2006 (38 days)
COSMIC FM1	Dec 2006 – Jun 2009	none
COSMIC FM2	Dec 2006 – Jun 2009	30 Jul 2008 (38 days)
COSMIC FM3	Dec 2006 – Jun 2009	18 Feb 2008 (43 days)
COSMIC FM4	Dec 2006 – Jun 2009	none
COSMIC FM5	Dec 2006 – Jun 2009	none
COSMIC FM6	Dec 2006 – Jun 2009	9 Sep 2007 (66 days)
METOP-A	May 2008 – Jun 2009	none

uncorrelated. However, there is evidence that vertical correlations and anti-correlations exist in the data, as shown from simulations (Syndergaard, 1999; Steiner and Kirchengast, 2005) as well as from actual observation data (Poli et al., 2009). Yet, turning these results into a realistic observation error covariance matrix that would improve the performance of GPSRO data assimilation remains a difficult task.

The GPSRO data quality controls (QC) are as follows. First, a gross QC removes observations located above 40 km impact height. This is to limit analysis increments in the upper region of the 60-level model where the vertical resolution is coarse (spacing between levels exceeds 2–3 km). The data marked as bad by the data provider are also removed (when the relevant quality indicator is available).

For MetOp-A GRAS data, the gross QC also removes data below 10 km (all data below 8 km) impact height in the tropics defined here as the latitude band 20°S–20°N (respectively, extratropics). The geometrical optics method, which is so far applied to process MetOp-A GRAS data, has indeed been shown to cause biases in the troposphere with CHAMP data (Ao et al., 2003).

Second, the data are subject to a background (or first-guess) check. This QC rejects observations that present departures with the background equivalent that exceed approximately nine times the prescribed observation error standard deviation.

Unlike other satellite data assimilated in ERA-Interim, there is no redundancy (or thinning) QC applied to GPSRO data on top of that already applied by the data provider. All the GPSRO observations may be assimilated, independently of whether two of them are very close in time and in the spatial domain.

Finally, the variational QC (Anderson and Järvinen, 1999) is applied to the GPSRO data during the assimilation.

4 GPSRO Data Usage

This section considers the numbers of GPSRO data assimilated, as compared to other meteorological data available, to produce the ERA-Interim upper-air 4D-Var analyses.

Table 4.1 shows the bulk of available and used observations in ERA-Interim is provided by satellites: atmospheric motion vectors deduced from satellite imagery, ozone retrievals, and passive radiances collected by infra-red and micro-wave radiometers onboard weather satellites. These satellites are operated mostly by the U.S. National Oceanic and Atmospheric Administration (NOAA), the U.S. National Aeronautics and Space Administration (NASA), and Eumetsat.

Over the whole time period, the number of available GPSRO data appears as a small fraction of the total number of data available. This is primarily because GPSRO data were only available from 2001 onwards. Also, even when GPSRO data are the most numerous (as of 2009), the daily GPSRO data count (on the order of 0.7 million) is quite small compared to satellite radiances or satellite winds (on the order of 100 million).

Although not shown in the table, between 1989 and 2009, the number of data available for ERA-Interim increased slowly for nearly all the observation types. This is especially the case for satellite data, whose number was multiplied by a factor 10 between the 2000 and 2003. In general, this increase is explained by the deployment of new sensors (surface stations, aircraft, satellite) but also by equipment upgrades allowing for more measurements (or higher spectral resolution) at each site or from each instrument. However, note that, over the same time period, the number of radiosonde sites actually decreased; this was compensated in terms of total data count by equipment upgrades at the remaining sites that allowed for measurements to reach higher in the stratosphere.

Table 4.1 shows a large drop between the total number of available data (557 billion) and the number of data passed to the assimilation (29 billion). There are several reasons to that. First, all data are subject to gross, redundancy, and background QCs before assimilation. Second, many data simply cannot yet be assimilated. In ERA-Interim, this is the case for cloud-contaminated satellite infra-red radiances. In fact, on any given day, most of the Earth is covered by at least a small fraction of clouds if one considers a pixel that is several km in size (which is about the resolution of past and current satellite radiometers). Efforts are underway to improve the use of cloud-affected infra-red data. For example, since ERA-Interim, the ECMWF operational NWP system has been upgraded to assimilate cloud-affected infra-red data in completely overcast regions (McNally, *Personnal Communication*). For micro-wave radiance data, all data likely to contain a surface signal were also systematically rejected in ERA-Interim over land due to uncertainties in the surface land emissivity. This point is also an area of current research (Karbou et al., 2007).

On average over the entire time period, only 5% of the available satellite and ozone retrieval data were passed to the assimilation. The highest mean daily usage rate is that of GPSRO data, at about 60%, followed by radiosondes, at about 50%. Note that for radiosondes, another reason to discard data are when they report the same information: the wind speed

Table 4.1: Observation data count (millions) in ERA-Interim between 1 January 1989 and 31 December 2008. 'Assimilated data' are data that passed gross QC, background QC, and redundancy QC

Data-type label and definition	Count of data available (assimilated)	Mean daily usage rate
PAOB: Australian surface pressure pseudo-obs	5 (0)	0%
DRIBU: drifting buoy data	184 (52)	28%
LIMB: GPSRO bending angle data	441 (319)	61%
PILOT: wind profilers and weather balloons reporting wind data only	790 (441)	53%
TEMP: radiosonde data (temperature, wind, humidity)	1913 (953)	49%
AIREP: aircraft data	2619 (1188)	42%
SCATT: scatterometer wind data	2838 (765)	32%
SYNOP: surface and ship data	3209 (478)	15%
SATOB: satellite wind data	12631 (718)	19%
SATEM: satellite passive radiance and ozone retrieval data	532684 (24141)	5%
TOTAL: All data	557314 (29056)	6%

and direction are redundant with the zonal and meridional components of wind; geopotential height is redundant with temperature (given pressure, assuming hydrostatic equilibrium); and relative humidity is redundant with specific humidity (given temperature and pressure).

The numbers of data assimilated shown in Table 4.1 correspond in fact to data presented to the assimilation; some of these data may have been rejected during the assimilation by the variational QC. For GPSRO, this is the case for about 0.4% of the data. This number is comparable to those found for the other observation types.

The time evolution of the GPSRO daily data usage is as follows. When only CHAMP data are available (May 2001–Dec 2006), the usage rate of GPSRO data is between 97–99%. When COSMIC data become available (around the end of 2006), the GPSRO data usage decreases to about 90%, because COSMIC probes lower in the troposphere (especially in the tropics) than CHAMP. The data collected there are thus more prone to background QC rejection. Possible reasons for background QC rejection are strong ducting or super-refraction that would have affected the data quality in the moist lower troposphere, or the inability of the model to reproduce the strong refractive index gradient seen by the fine vertical resolution of GPSRO. Then from mid-2007 onwards, the vertical coverage of COSMIC data was extended at the top by UCAR CDAAC from 40 km to 60 km. Because all these additional GPSRO data are rejected by gross QC, the effective GPSRO data usage fell by about a third, to about 60–65%. As of mid-2009, this usage rate remains among the largest as compared to other observations.

5 Comparison of GPSRO Data with ERA-Interim

This section considers time-series of statistics of differences between GPSRO bending angle observation (y^0) and the background equivalent ($H(x_b)$), over the 8-year time period during which GPSRO data have been assimilated, between May 2001 and June 2009. Note that H denotes the GPSRO observation operator and x_b is the background obtained by a forecast integration (from the previous analysis) discretized in one-hour time-slots. The GPSRO background relative departures discussed here are defined as $[100 * (y^0 - H(x_b))/y^0]$.

Figure 5.1 shows the global mean of this quantity, calculated daily and with a vertical binning of 1 km. The vertical structure appears stable over time, indicating persistent, systematic differences between ERA-Interim and GPSRO observations. Larger systematic relative differences are observed in the lower troposphere where more moisture is present. A break can be seen around end 2006, when additional GPSRO data (COSMIC) were introduced. The assimilation of more GPSRO data apparently had the effect of bringing the re-analysis closer to GPSRO data. This is most visible around 12–16 km impact height.

The standard deviations of the observation minus background relative differences are shown in Figure 5.2. They are much larger (a few percents) than the mean relative departures, which are on the order of 1 percent. This a posteriori check is consistent with the assimilation of GPSRO data without bias correction. The standard deviations also decrease steadily over time. That decrease is sharp when COSMIC data are introduced (end 2006) but is also visible in the years before. Since the number of CHAMP data was relatively stable between 2001 and 2006, the likely reason for this decrease is the improving quality of the ERA-Interim re-analysis, which assimilated a growing number of other satellite data (in particular radiances from the Advanced Microwave Sounding Unit-A, AMSU-A, introduced in 1998).

Looking now over the tropics only (latitudes 20°S–20°N), we can spot in Figure 5.3 in the stratosphere a downward-propagating pattern between impact heights 32 km and 20 km. A similar signature is obtained by inspecting mean GPSRO analysis relative departures. This signature matches the time pattern of the Quasi-Biennial Oscillation (QBO). This oscillation affects the equatorial stratospheric zonal winds. Its effect on GPSRO data had already been identified by Schmidt et al. (2004) who inspected anomalies in GPSRO temperature retrievals in the latitude band 4°S–4°N. Further study is required to explain the QBO representation in GPSRO bending angle.

In order to evaluate the inter-satellite consistency of the GPSRO data, Figure 5.4 shows the time-series of the mean observation minus background relative differences for each satellite in the Southern Hemisphere extratropics (SH, latitudes 20°S–90°S). The results are binned in the vertical in five broad vertical layers. These same layer definitions are used later to compare ERA-Interim with radiosonde and aircraft temperature observations. In the lowest layers, the CHAMP data exhibit a larger bias as compared to the background than the COSMIC data. This difference could be the result of a different sampling of the atmosphere as COSMIC probes regularly more often lower in the troposphere. For the layers above 8 km impact height, we note the consistency between CHAMP and COSMIC. That consistency is

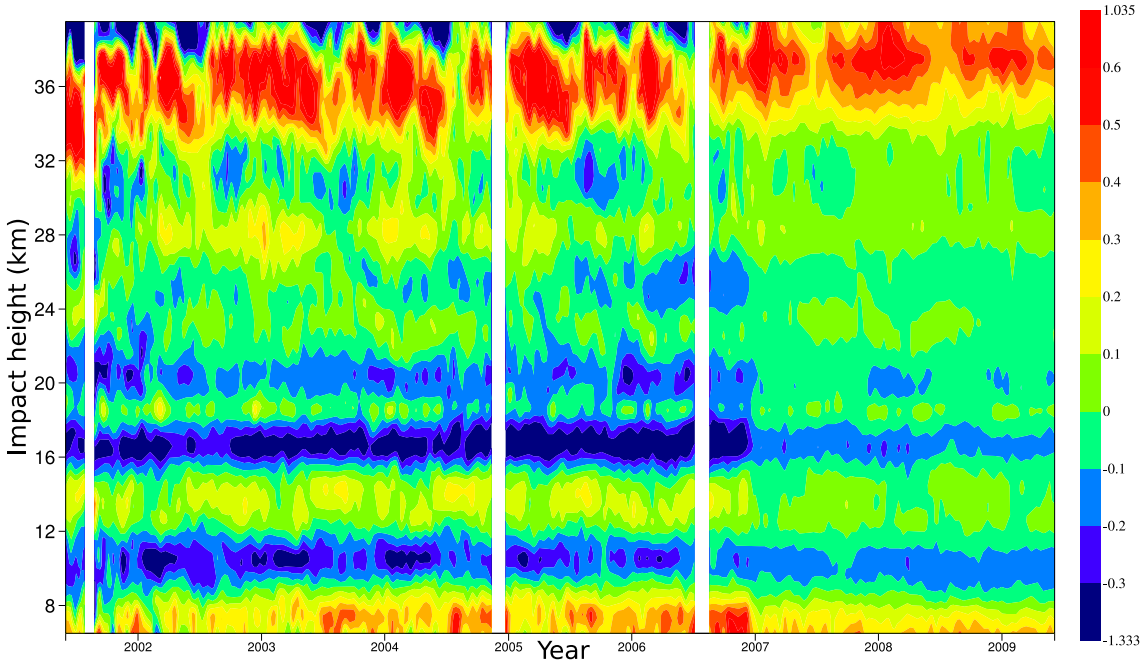

Figure 5.1: Mean of the GPSRO background relative departures (percents)

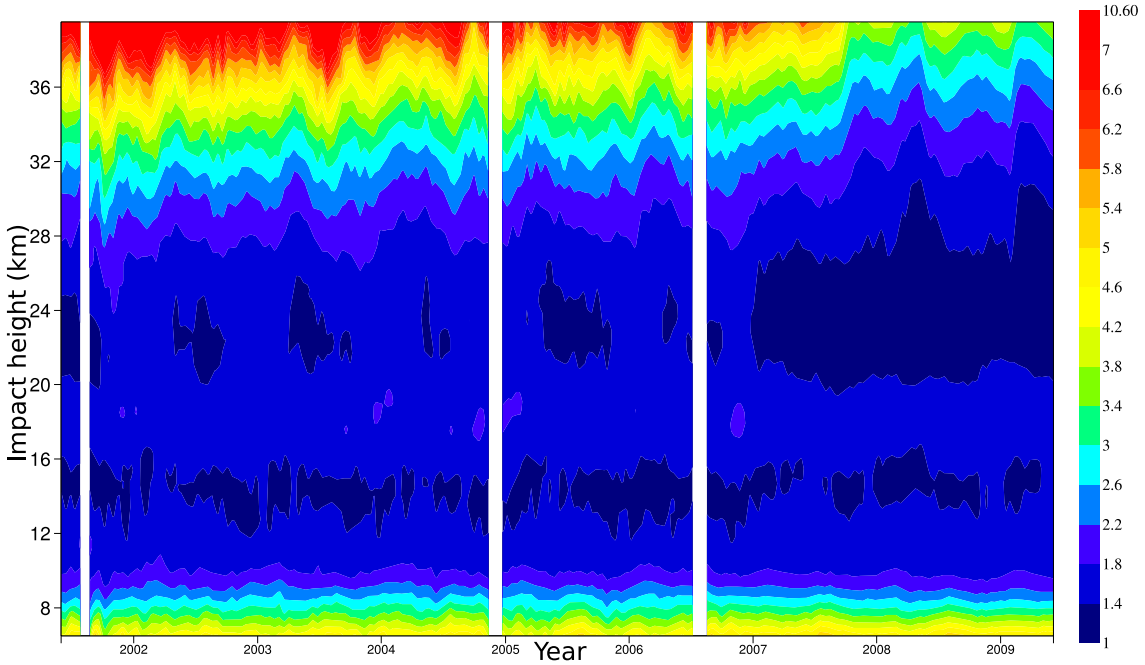

Figure 5.2: Same as Figure 5.1, but for standard deviation

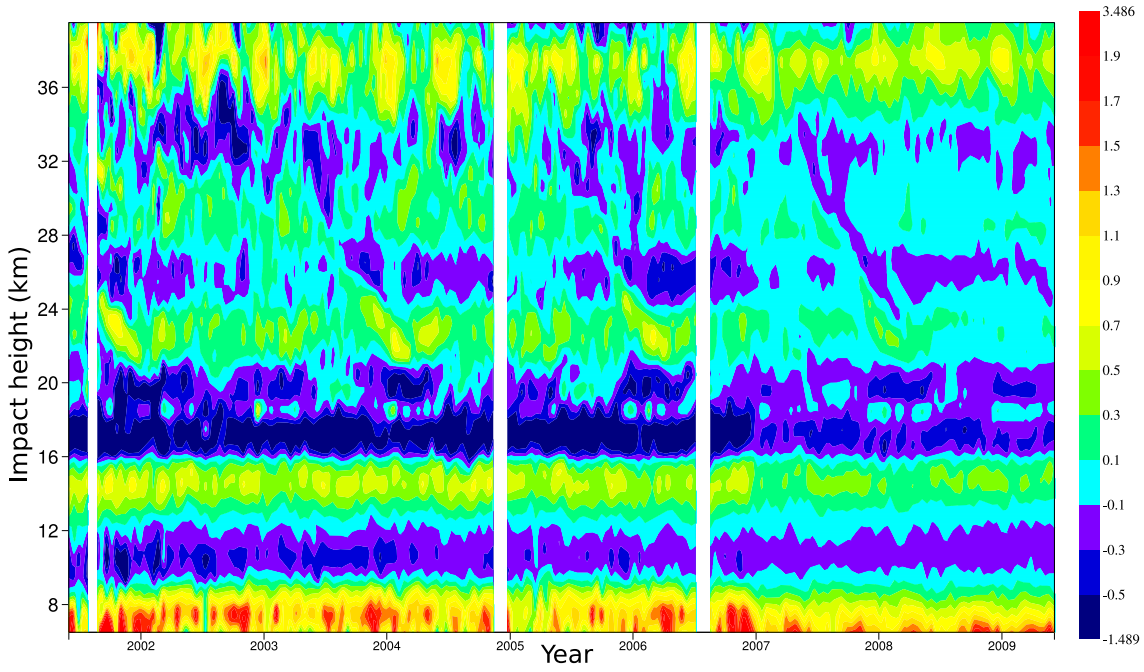

Figure 5.3: Same as Figure 5.1, but for the tropics (latitudes 20°S–20°N). Note the downward-propagating patterns between 32 km impact height and 20 km impact height in 2002, 2004, 2006, and 2008

all the more remarkable given that the GPSRO data are assimilated without bias correction of any sort. The mean statistics for GRAS stand out from those for CHAMP and COSMIC for the tropopause and lower stratosphere layer (13–20 km); the mean differences between ERA-Interim and COSMIC data are smaller than between ERA-Interim and GRAS. This is a known difference already reported by NWP monitoring and that may be addressed by changes at one of the data provider's side. We observe that the mean relative background departures are closer to zero for CHAMP in the highest layer (13–20 km) after the introduction of COSMIC data end 2006. This reduction thus reflects changes in the background following the assimilation of COSMIC data in ERA-Interim and is consistent with Figure 5.1.

In the Northern Hemisphere extratropics (NH, latitudes 20°N–90°N), Figure 5.5 shows similar results with the additional remark that statistics for GRAS appear as slightly different from those for CHAMP and COSMIC around 8–10 km in 2008. This may be explained by changes in processing at Eumetsat during 2008 (the first year of processing GRAS data).

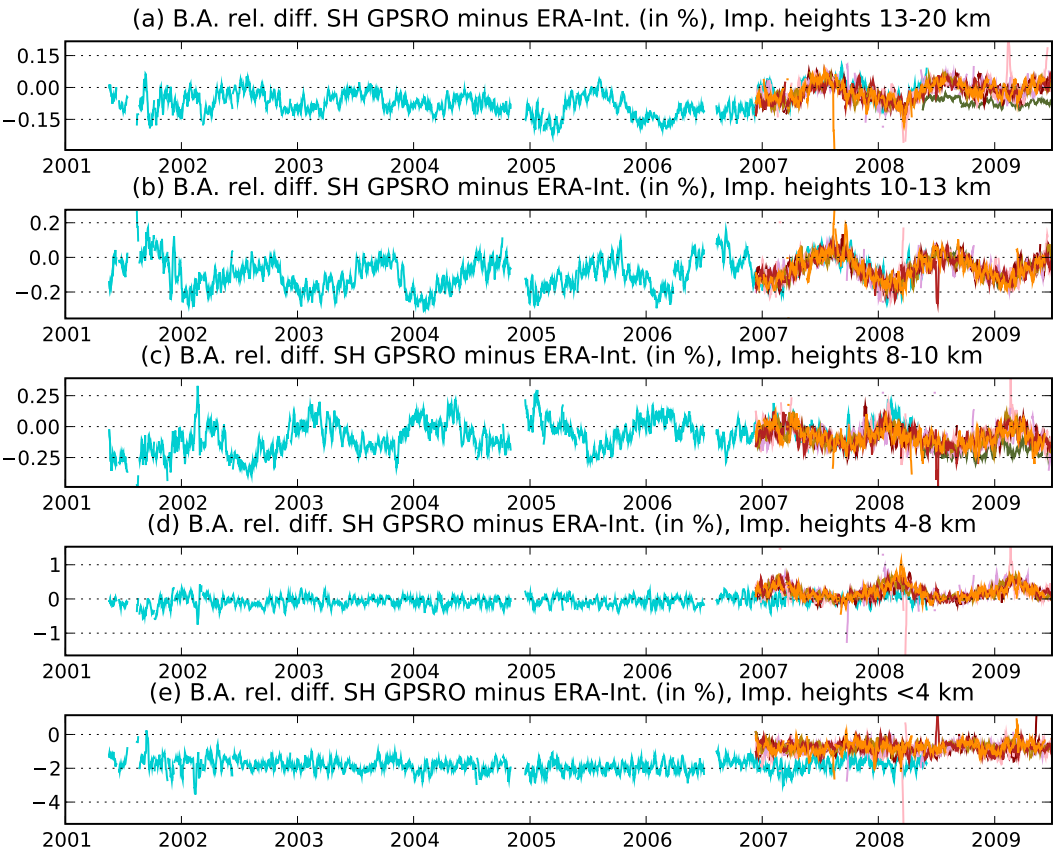

Figure 5.4: Mean of the mean daily GPSRO background relative departures (in percents of observed bending angle), in the Southern Hemisphere extratropics (SH) for different layers defined in terms of impact height. Light blue (green) shows statistics for CHAMP (GRAS on MetOp-A); the warm colors (red, orange, ...) correspond to the various COSMIC satellites (-1 to -6). The resuts are smoothed using a seven-day moving average to enable comparison between the satellites

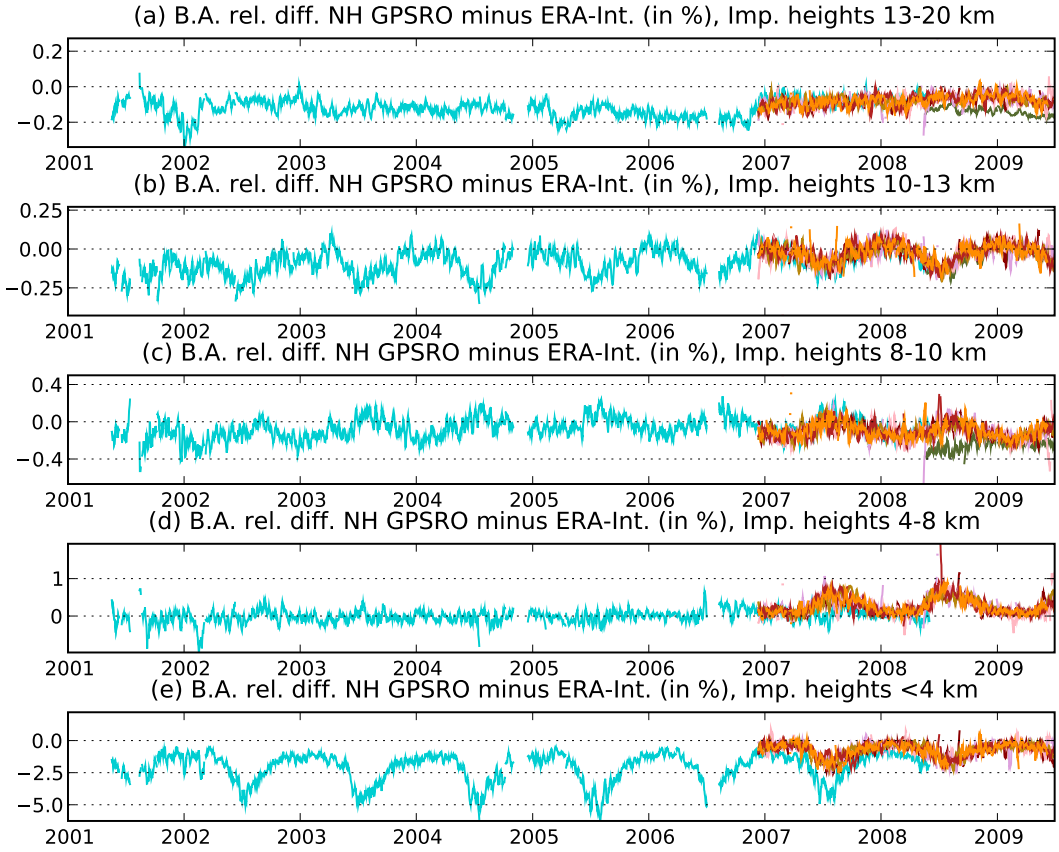

Figure 5.5: Same as Figure 5.4, but for the Northern Hemisphere extratropics (NH)

6 Possible Impact of GPSRO Data as Inferred from Observed Changes in ERA-Interim Time-series

Assessing the impact of a change in computer, NWP model, or data assimilation scheme from changes in the behavior in data assimilation system-produced time-series is a common practice at NWP centers as regards the evolution of forecast scores. These scores are indeed regularly scrutinized to monitor improvement. However, it is sometimes difficult to discerne in these evolutions the effect of a recent upgrade shortly after it has taken place. Indeed, some of these upgrades take time to give their full effects. However, in retrospect, this exercise typically proves much easier when long time-series are available. In such case, the changes in the mean behavior may stand out from the natural variability that permanently affects all weather-related time-series.

We apply a similar heuristic approach to investigate the possible impact of GPSRO data assimilation in ERA-Interim. We focus our search on one particular event (E): the introduction of COSMIC data on 12 December 2006, at which point the number of GPSRO data assimilated suddenly increased by an order of magnitude, from about 30,000 per day to about 350,000 per day.

Important caveats apply to conclusions drawn from that method. The suspected changes may be related to other changes in the observing system and/or the natural variability.

Figure 6.1 shows time-series of the mean of radiosonde temperature minus ERA-Interim background for the approximately same layers as defined in terms of impact height in the previous section, over the Southern Hemisphere extratropics continents. The differences between the red and blue curves are a good estimation of how much bias exist between the ERA-Interim system and the observations, and whether these observations force ERA-Interim to fit the mean observations. Event (E) seems related to a change in the mean first-guess fit to radiosondes at the tropopause and lower stratosphere layer (pressure levels 175–60 hPa). Before (E), the first-guess presents a cold bias (about 0.2 K) at these levels; after (E), it seems that this bias is reduced to near-zero. Looking in more detail, this effect is more pronounced for the particular layer 125–85 hPa (not shown). This is consistent with the introduction of COSMIC data in the ECMWF operational model at the time (Luntama et al., 2008).

One new finding in the present study is that this effect is not only limited to the Southern Hemisphere, where the observing system is otherwise sparse in terms of vertically resolved temperature observations. Figure 6.2 shows similar statistics for the Northern Hemisphere, which is by experience quite difficult to affect with satellite data, for it remains closely tied to radiosonde observations. The cold background bias of 0.2 K as compared to radiosondes over land is reduced to near-zero after (E). Similar results (not shown) indicate a similar impact in the tropics, with a background cold bias reduction around the lower stratosphere and tropopause layer (in particular in the layer 125–85 hPa, from 0–0.6 K before (E) to -0.3–0.3 K after (E)).

Figure 6.3 shows time-series of differences between aircraft temperatures and ERA-Interim

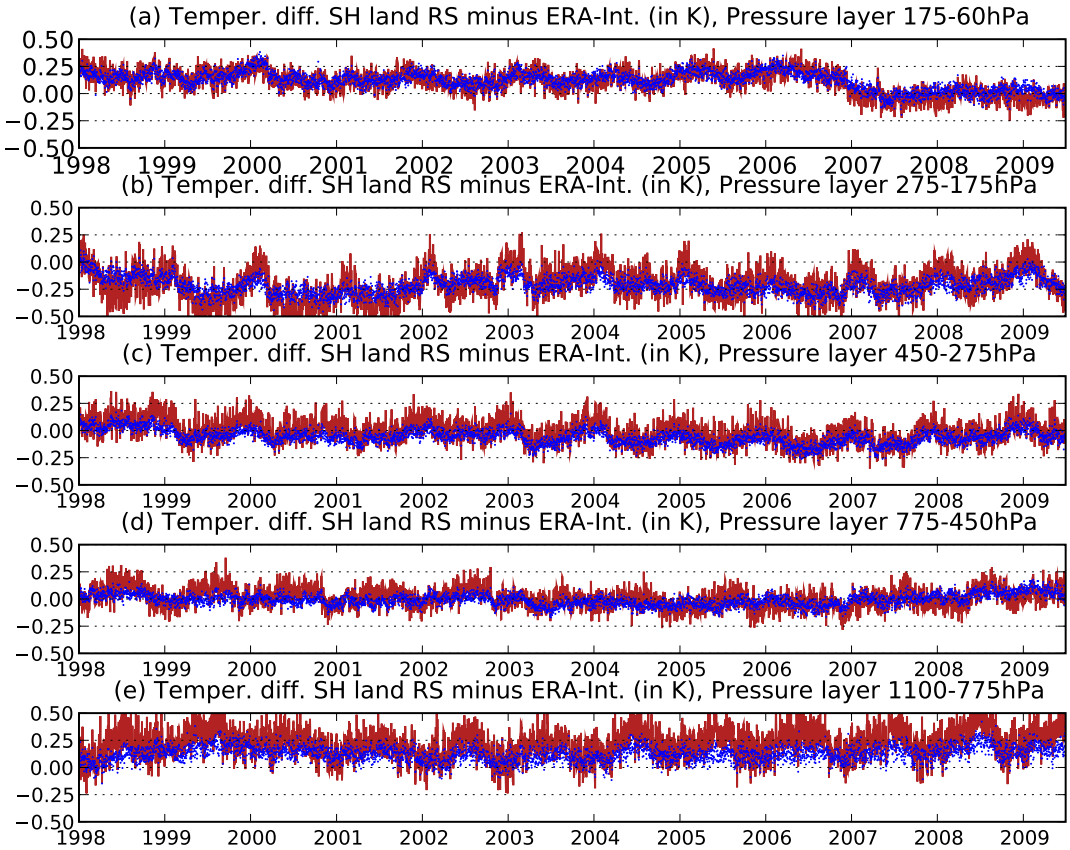

Figure 6.1: Time-series of daily radiosonde temperature (in K) observation minus ERA-Interim background (in red) mean difference over land in the Southern Hemisphere extratropics, for five different pressure layers that correspond approximately to the impact height layers shown in Figure 5.4. Differences with respect to ERA-Interim analyses are shown with blue dots

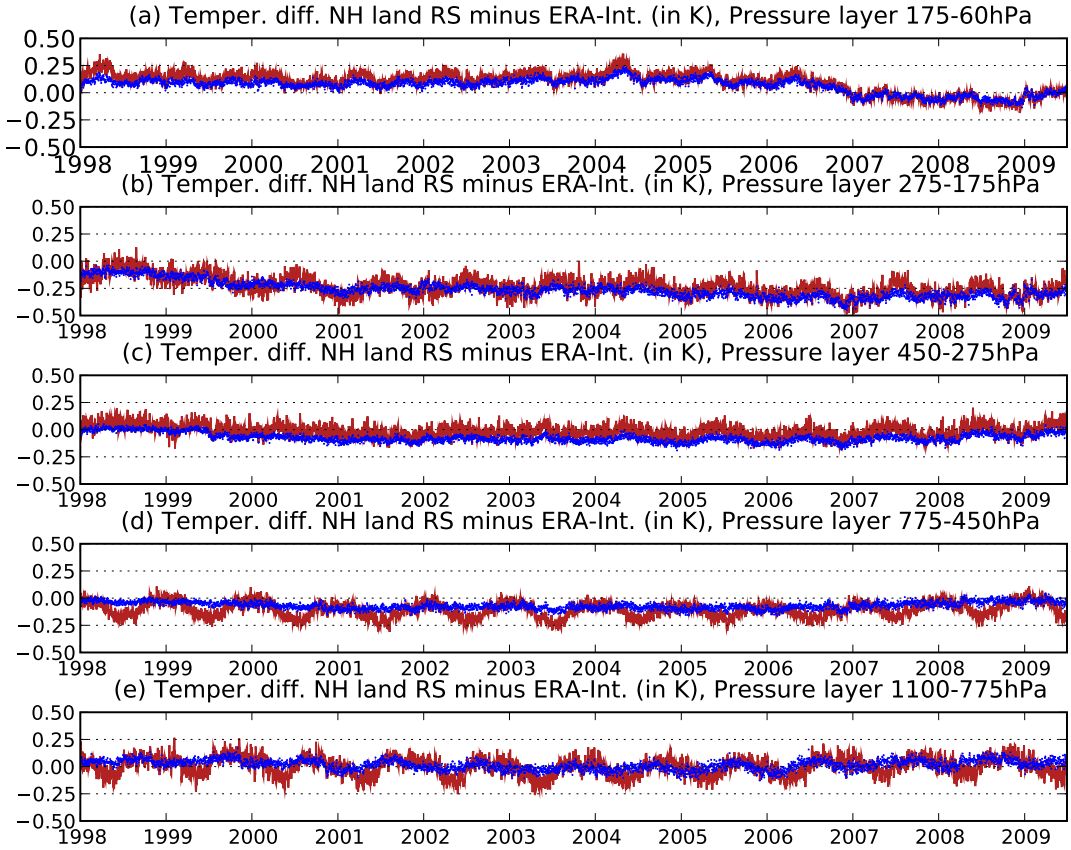

Figure 6.2: Same as Figure 6.1, but for the Northern Hemisphere extratropics

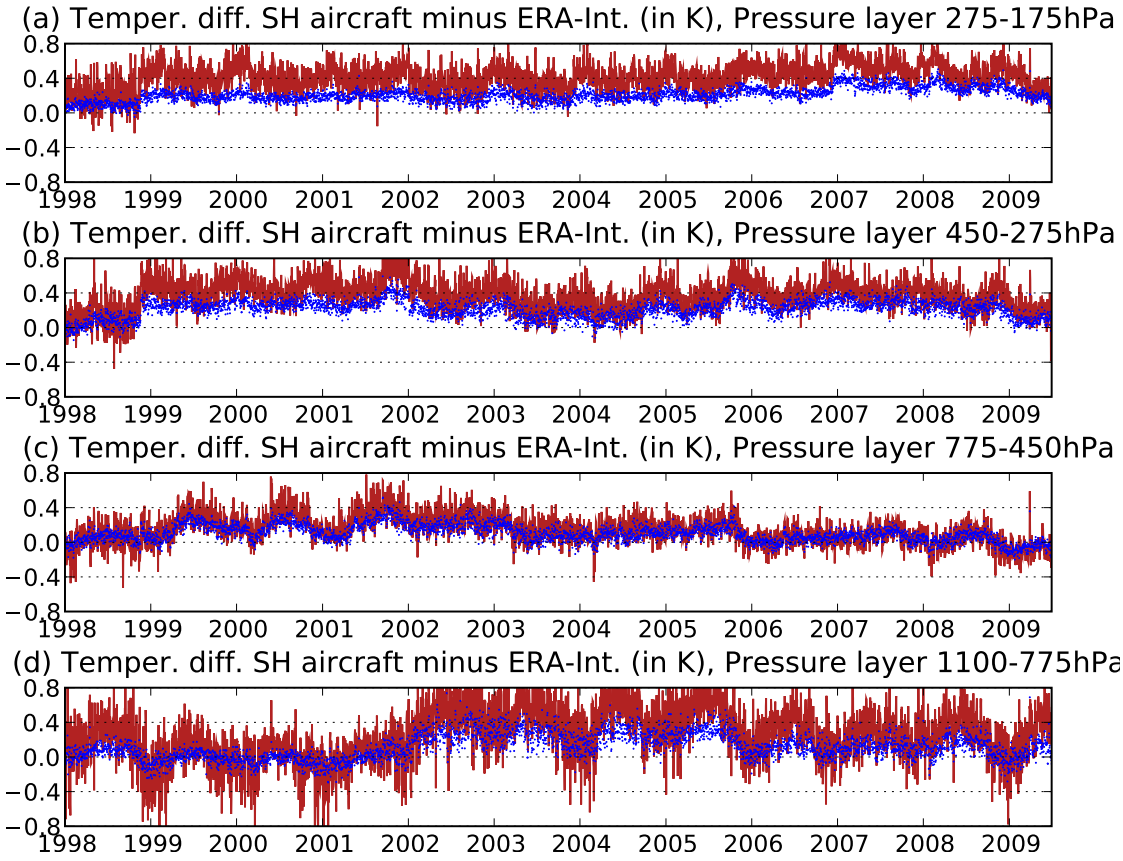

Figure 6.3: Same as Figure 6.1, but for aircraft observations (note: only four layers are shown, because of too few aircraft data for the layer 175–60 hPa)

background and analysis. We note that (E) seems related with an increase in the mean differences for the layer 275–175 hPa. After (E), ERA-Interim does not fit as much the aircraft temperature observations (mean analysis differences increased from 0.1 K before (E) to 0.3 K after (E)). The aircraft data at this level (long-haul flight cruising altitude) have been shown to present a warm bias as compared to the radiosonde observations as noted earlier by Dee and Uppala (2009).

Looking now for a possible impact of GPSRO observations on the humidity in the reanalysis, Figure 6.4 suggests a possible change in the tropics (latitude 20°S–20°N) over land related with (E). The background bias seems to be shifted towards a drier regime (as compared to radiosondes) for the layers 1100–775 hPa and 775–450 hPa after (E). However, another possible cause for the change in mean humidity fit to radiosondes is the introduction of Meteosat geostationary radiance assimilation around mid-2006. These data are indeed known to bring information about the tropospheric water vapor content.

The time-series of departures between ERA-Interim background and radiosonde observations shown in this section suggest possible impacts of the introduction of COSMIC data, on temperature around the tropopause and on humidity in the tropical lower troposphere. There is quite some confidence in the case of temperatures around the tropopause because it matches earlier findings. However, there are some doubts about the humidity impact as it could also be the result of the introduction of Meteosat radiances.

To clarify these points, an observing system experiment has been conducted, focusing on

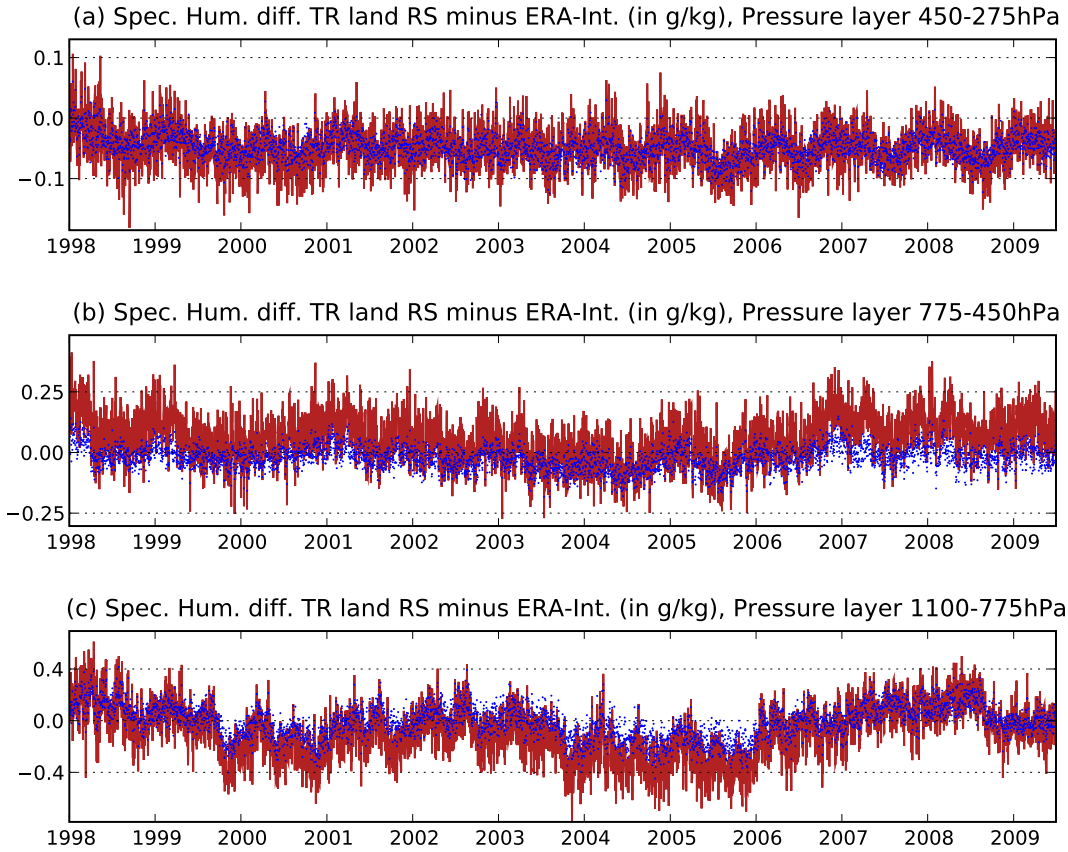

Figure 6.4: Same as Figure 6.1, but for the specific humidity (in g/kg) in the tropics, and the bottom three pressure layers

the time period after event (E).

7 Observing System Experiment with the ERA-Interim System

We now present results of a data withholding experiment to assess the impact of GPSRO data in the more recent years of ERA-Interim (after the introduction of COSMIC). The first experiment (control, denoted CTRL), from 1 December 2008 to the end of February 2009, uses nearly the same system as the ERA-Interim re-analysis. The only difference is that the sea surface temperature (SST) input throughout the period come from the National Centers for Environmental Prediction (NCEP), whereas in ERA-Interim the SST input was changed from the NCEP SST product to the Operational Sea Surface Temperature and Sea Ice Analysis (OSTIA) SST product on 1 February 2009. The second experiment (denoted as NOGPS) reproduces CTRL over the same time period, with the difference that no GPSRO data is assimilated (the GPSRO data are rejected in the gross QC step).

7.0.1 Impact on temperature

The mean temperature differences between CTRL and NOGPS are shown in Figure 7.1. The magnitudes of the average differences are at most 0.4 K, near the tropopause. The net effect of assimilating GPSRO data is to increase the temperatures by about 0.1–0.2 K globally around the 100 hPa pressure level, and to reduce the temperatures below that level (from a 0.1–0.2 K reduction around the 200 hPa pressure level to near-zero near the surface). Also, by looking at the dipole pattern at pressure levels 100 hPa and 200 hPa, we further postulate that the removal of GPSRO data may displace slightly the tropopause in the vertical, locating it slightly higher. Note that the GPSRO data do not only change the mean state; the standard deviation of the differences CTRL minus NOGPS is up to 0.8–0.9 K, above the 200 hPa pressure level.

We now consider Figure 7.2 which shows the mean of radiosonde temperature observation minus background over land in the Northern Hemisphere extratropics, for the two experiments. We find here a confirmation of the increments shown in Figure 7.1: assimilating GPSRO data has a warming effect around the 100 hPa pressure level (up to 0.2 K), and a cooling effect (though smaller) in the entire troposphere. We find similar results in the Southern Hemisphere extratropics and the tropics (not shown). Note that we do not have sufficient validation data to confirm the similar conclusions over the ocean.

We conclude that the introduction of large numbers of GPSRO data around end 2006 had a two-fold impact on ERA-Interim temperatures:

- a warming of by about 0.1–0.2 K at the tropopause and in the lower stratosphere; this also brought ERA-Interim closer to radiosonde observations, but also caused a discontinuity in ERA-Interim temperature products at these levels,
- a cooling in the troposphere, especially around the 200 hPa pressure level; however this cooling is not readily visible on long ERA-Interim time-series comparisons with

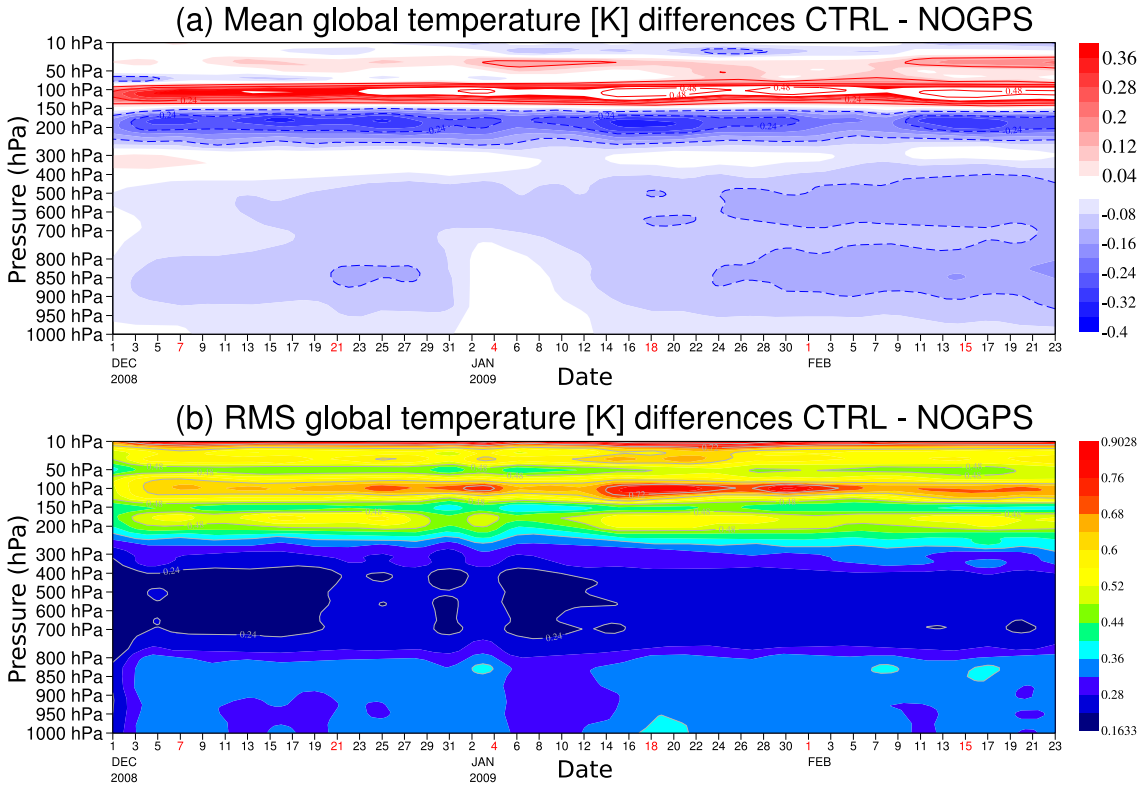

Figure 7.1: Mean and root-mean-square (RMS) temperature differences over the globe, between the ERA-Interim re-analysis (CTRL) and a similar run where GPSRO data are withheld (NOGPS)

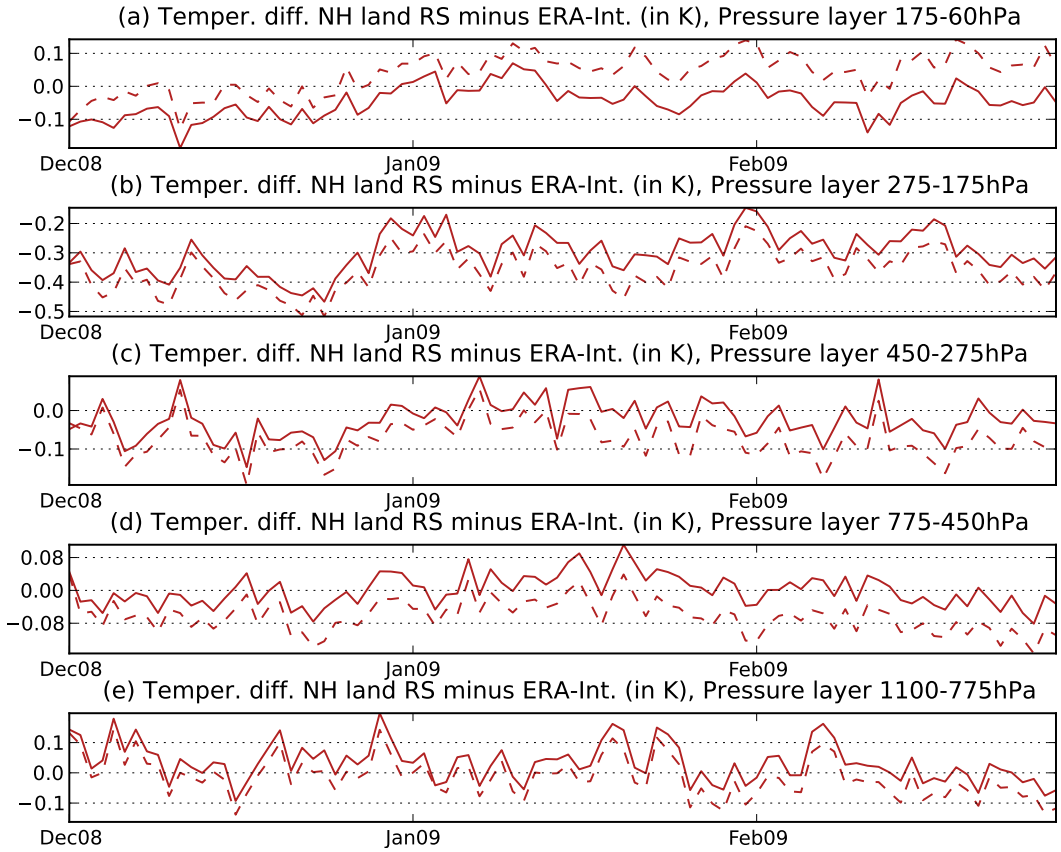

Figure 7.2: Same as Figure 6.2, but for the CTRL (solid line) and NOGPS (dashed line), only showing differences between observation and background

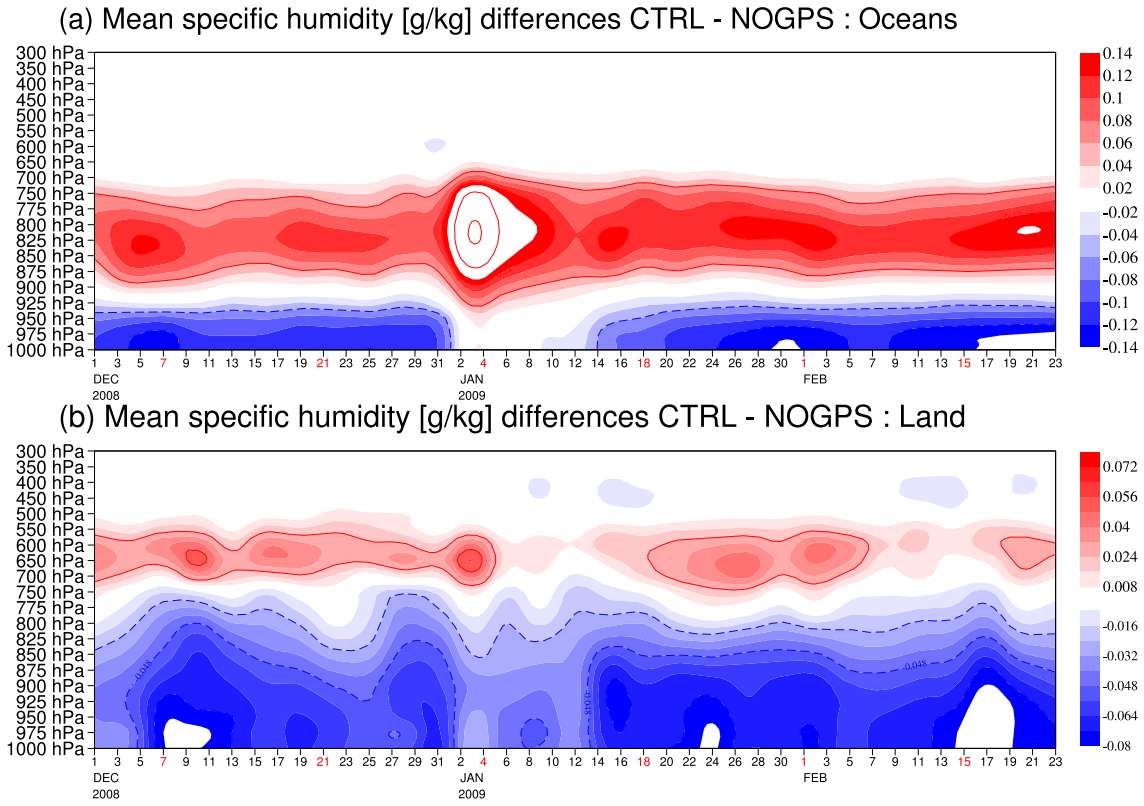

Figure 7.3: Same as Figure 7.1, but for specific humidity

radiosondes.

7.0.2 Impact on humidity

Figure 7.3 shows the specific humidity differences between CTRL and NOGPS. A large one-time difference is obvious on 2 January 2009 when new data were introduced in both experiments, namely the water vapor-sensitive channels from the Advanced Microwave Scanning Radiometer on the Earth Observing System (AMSR-E) Aqua satellite, and the Special Sensor Microwave/Imager-Sounder (SSMI/S) on the Defense Meteorological Satellites Program DMSP-16 satellite. Apparently the two experiments did not quite react in the same manner in the few hours following the introduction of these new data. Apart from that one-time difference, the mean effect of GPSRO data seems to be a moistening around the 800 hPa pressure level above the oceans, with a drying effect underneath. Over land, the moistening occurs at a higher altitude (around the 600 hPa pressure level). Differences in terms of simulated cloud coverage from the two experiments (not shown) show similar results, with essentially a drier lower troposphere and fewer low clouds when GPSRO data are included.

We now consider Figure 7.4 which shows the mean of radiosonde humidity observation minus background over land in the tropics, for the two experiments. For the lowest layer, the effect of adding GPSRO data is not so clear; looking however in the Northern and Southern extratropics (not shown), we find that the curve showing observation minus CTRL is usually located above that showing observation minus NOGPS, meaning that the humidity amount in CTRL is lower than in NOGPS (adding GPSRO data has a drying effect in the lowest layers).

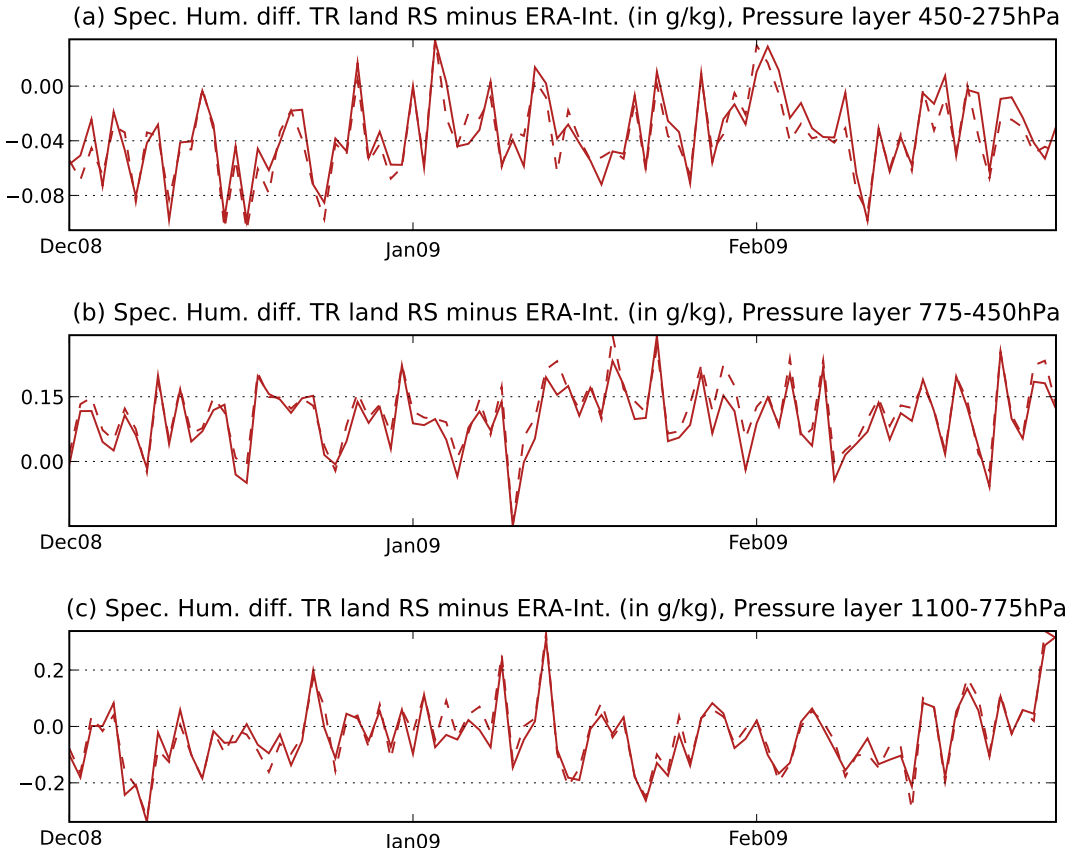

Figure 7.4: Same as Figure 6.4, but for the CTRL (solid line) and NOGPS (dashed line), only showing differences between observation and background

The opposite is true for the layer 775–450 hPa (adding GPSRO data has a moistening effect in the mid-troposphere). These two results are consistent with the global increment plots over land shown in Figure 7.3. Note that we do not have sufficient validation data to confirm the similar conclusions over the ocean.

Trying now to relate these findings with the earlier intuitive results seen from changes in the ERA-Interim time-series (previous section), we find a consistency for the drying effect in the lowest layer over land. However, we did not observe in these time-series any change suggesting a moistening in the layer 775–450 hPa. At best, these time-series exhibit an opposite trend, probably because of the introduction of Meteosat radiances.

To conclude, the impact on humidity of assimilating large numbers of GPSRO data in ERA-Interim (i.e. after the addition of COSMIC data) is two-fold:

- a drying of the lower troposphere, up to about 2.5 km altitude; this effect is even visible on long ERA-Interim time-series showing the fit to radiosondes over land; this results also in a discontinuity in ERA-Interim lower tropospheric humidity around end 2006;
- a moistening of the mid-troposphere, but this effect is not visible on long time-series (a likely explanation is that this effect was countered by the introduction of Meteosat radiances).

7.0.3 Impact on the assimilation of radiance data, via VarBC

Beyond the effect of GPSRO data on the mean re-analysis background state via the 4D-Var assimilation, there is another mechanism that extracts the information contained in GPSRO data. The VarBC applied in ERA-Interim corrects the radiance brightness temperatures using as a reference (or anchoring) all the other observations. In terms of vertically resolved temperature observations, the anchoring is then provided by radiosondes, aircraft, and GPSRO observations.

Figure 7.5 shows the time-series of mean bias corrections calculated by VarBC in both experiments, for a selection of AMSU-A channels and various satellites. The initial values are identical. It takes a few days for the effect of the removal of GPSRO data to become visible. The differences usually grow within a month and are larger in magnitude for AMSU-A channels 9–12 (peaking from the upper troposphere to the stratosphere, respectively). Looking at channel 5, one can also notice that the mean bias corrections, though nearly similar, diverge slowly for up to nearly two months after the removal of GPSRO data. This suggests some robustness of the re-analysis system in keeping the memory of the anchoring provided by GPSRO data.

Figure 7.6 shows the mean bias corrections for a few High Resolution Infrared Radiation Sounder (HIRS) channels calculated by VarBC. Again, the differences between CTRL and NOGPS take a few days to develop and become significant for HIRS channel 6 which peaks in the lower troposphere. No significant differences are observed for HIRS channels 11 and 12 (water vapor-sensitive channels).

We now consider again differences between radiosonde measurements and each experiment, searching for clues of the impact of GPSRO via VarBC on the mean fit. We thus leave out the first month of each experiment in this discussion since we saw that the effect of GPSRO data removal takes time to settle. Figure 7.7 shows these differences for

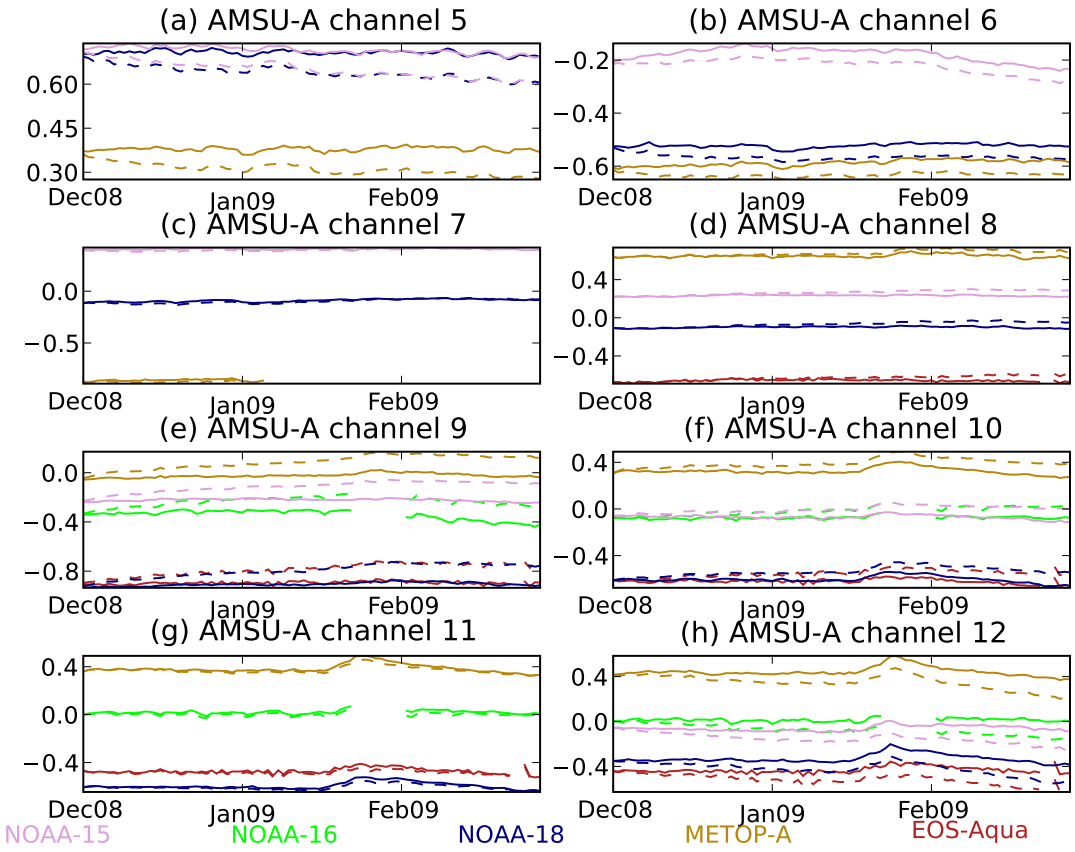

Figure 7.5: Time-series of daily mean bias corrections (radiance brightness temperature, in K) for a selection of AMSU-A channels on various satellites (indicated by different colors), calculated by VarBC in CTRL (solid line) and NOGPS (dash line)

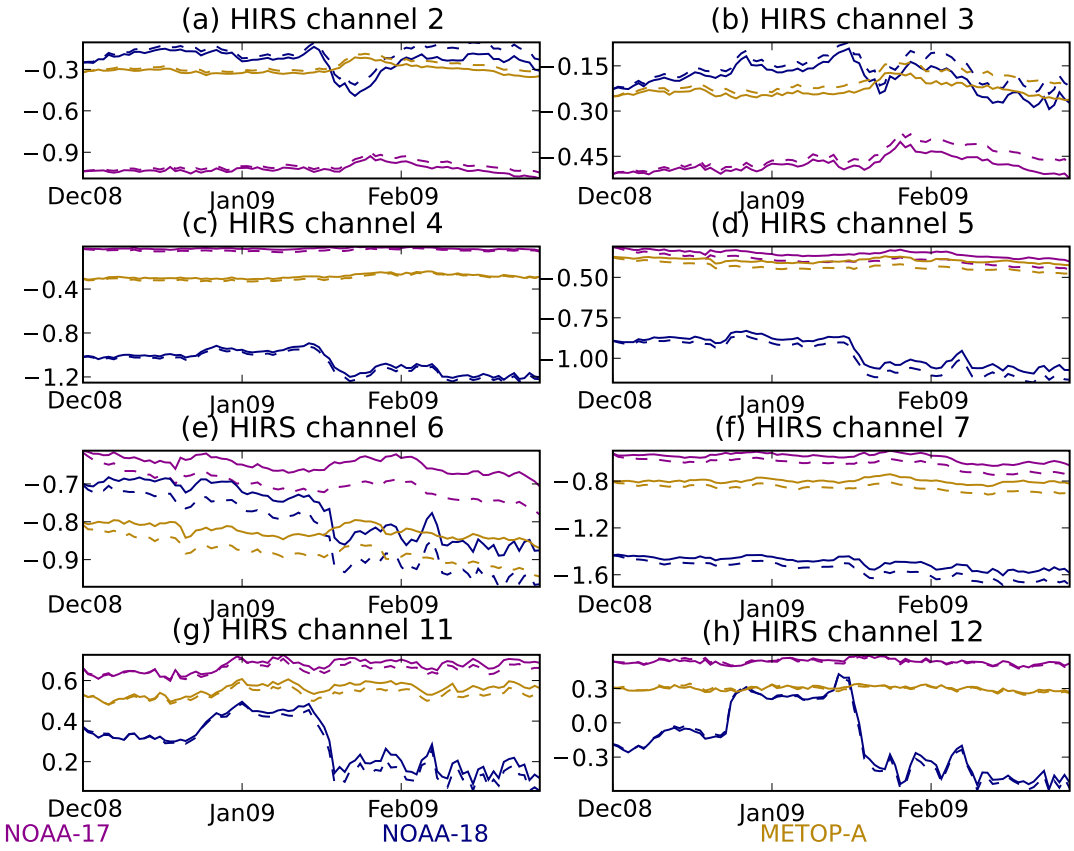

Figure 7.6: Same as Figure 7.5, but for a selection of HIRS channels

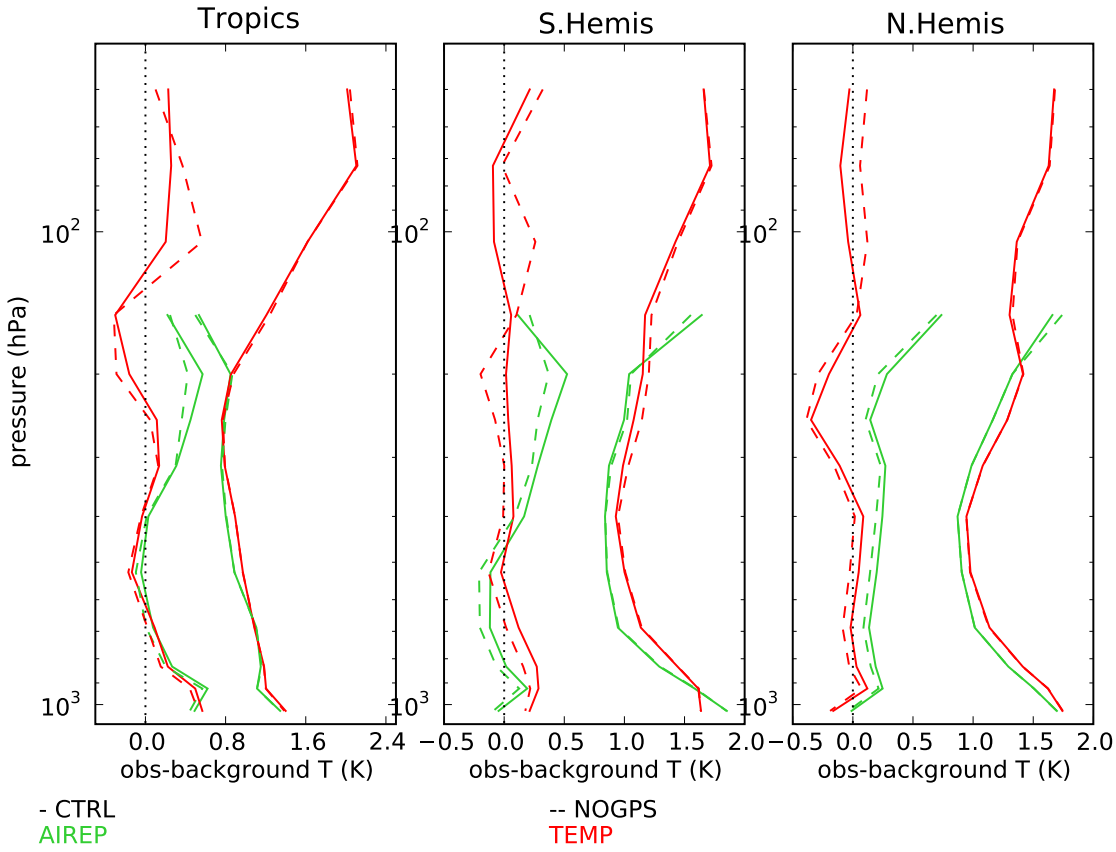

Figure 7.7: Mean (around the zero dotted line) and standard deviation of temperature differences (K) between in situ observations (aicraft, AIREP, and radiosondes, TEMP) and CTRL (solid line) and NOGPS (dashed line). Time period is January–February 2009

temperature, for three different latitude bands. The CTRL and NOGPS appear to be most significantly different at the 100 hPa pressure level. At that level, the CTRL is on average closer than NOGPS to radiosondes. The differences between radiosonde and NOGPS are positive for that level, meaning that NOGPS is colder than the radiosonde observations at 100 hPa (which themselves are more consistent with CTRL). The result NOGPS colder than CTRL at 100 hPa is consistent with Figure 7.1.

At the 200 hPa pressure level, we observe a different situation, NOGPS is still further away from the radiosonde observations than CTRL, but this time NOGPS appears to be warmer than CTRL. This is also consistent with Figure 7.1. At the 200 hPa level, ERA-Interim is in fact assimilating a significant number of aircraft data. Figure 7.7 shows the differences between aircraft temperatures and each experiment. The differences between CTRL and NOGPS appear most significant at the 200 hPa pressure level. At that level, CTRL is colder than aircraft temperatures by up to 0.5 K. We find that NOGPS is also colder than aircraft temperatures, but by a smaller amount. In fact, NOGPS is warmer than CTRL and more in agreement with the aircraft temperatures. We conclude from this discussion that the GPSRO data are in agreement with radiosondes at 200 hPa but disagree with aircraft data. These latter data are apparently too warm, as also found by Dee and Uppala (2009). Removing GPSRO data has the effect of allowing the upper-air re-analysis system to draw more to the aircraft data and results in a warmer 200 hPa region. Conversely, adding GPSRO data makes the background colder at 200 hPa and counter-acts against the warm aircraft

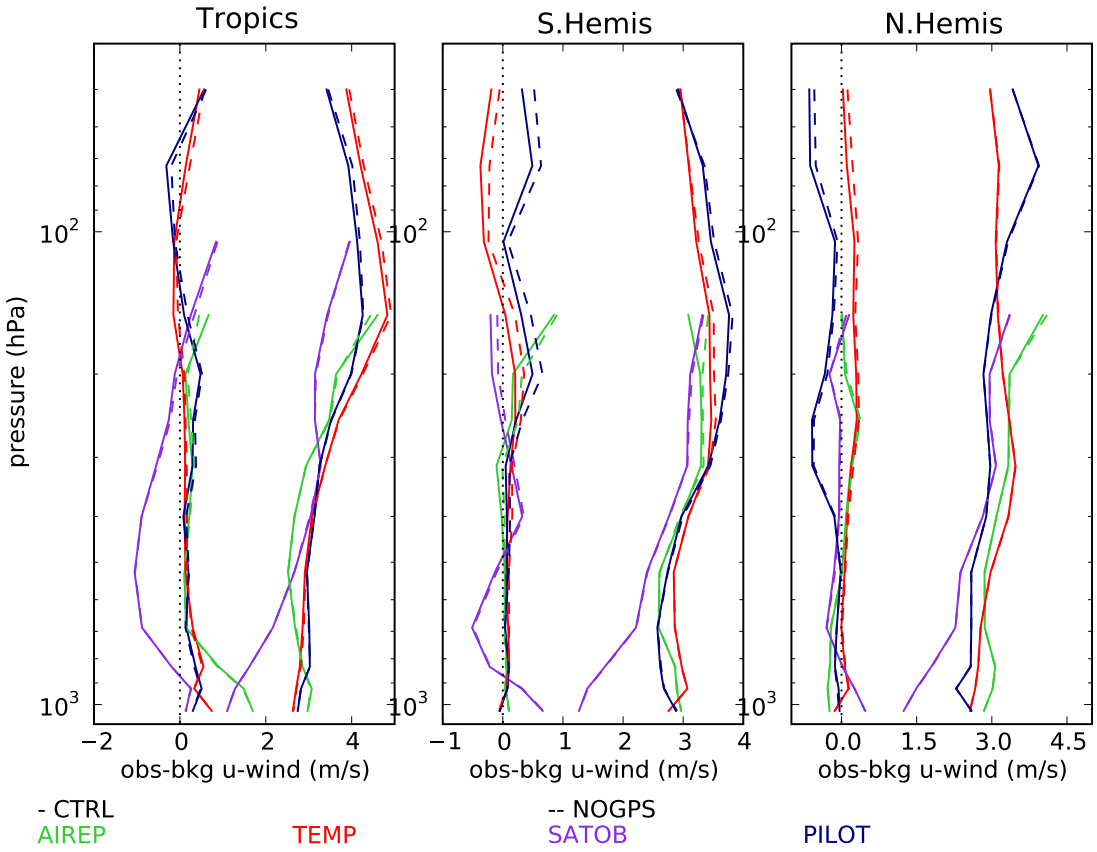

Figure 7.8: Same as Figure 7.7, but for zonal wind (m/s) measured by aircraft (AIREP), wind profilers and radiosondes reporting wind only (PILOT), radiosondes (TEMP), and satellite as inferred from satellite imagery (SATOB)

temperature observations.

7.0.4 Impact on the variability represented in ERA-Interim

The impact of GPSRO data on the variability represented in the re-analysis was briefly mentioned earlier when interpreting the RMS of the temperature differences between CTRL and NOGPS. Figure 7.7 shows that adding GPSRO data helps the re-analysis fit better the natural variations as estimated by the standard deviation of the differences with respect to aircraft and radiosonde observations.

Figure 7.8 shows the standard deviation of the differences between ERA-Interim and zonal wind observations. These differences are reduced when GPSRO data are present in the stratosphere and the upper troposphere in the Southern hemisphere and the tropics, with no visible impact in the Northern Hemisphere. We also observe that adding GPSRO data modifies slightly the mean differences in all areas in the upper troposphere and lower stratosphere. As compared to satellite winds and radiosonde observations, the GPSRO data appear to shift the mean zonal wind difference towards negative values. This suggests that the zonal winds at pressure levels 200–50 hPa in the background are increased with the assimilation of GPSRO data.

This result needs to be analysed in conjunction with the meridional wind fits to obser-

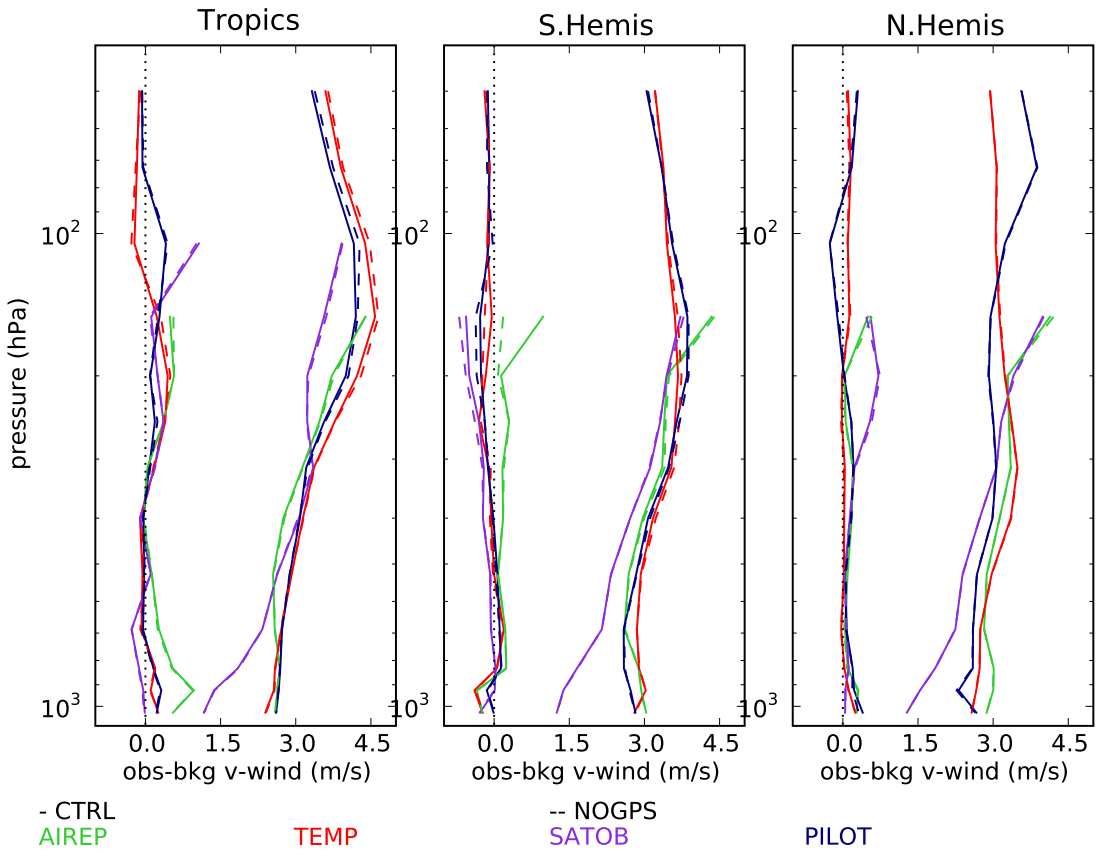

Figure 7.9: Same as Figure 7.8, but for meridional wind

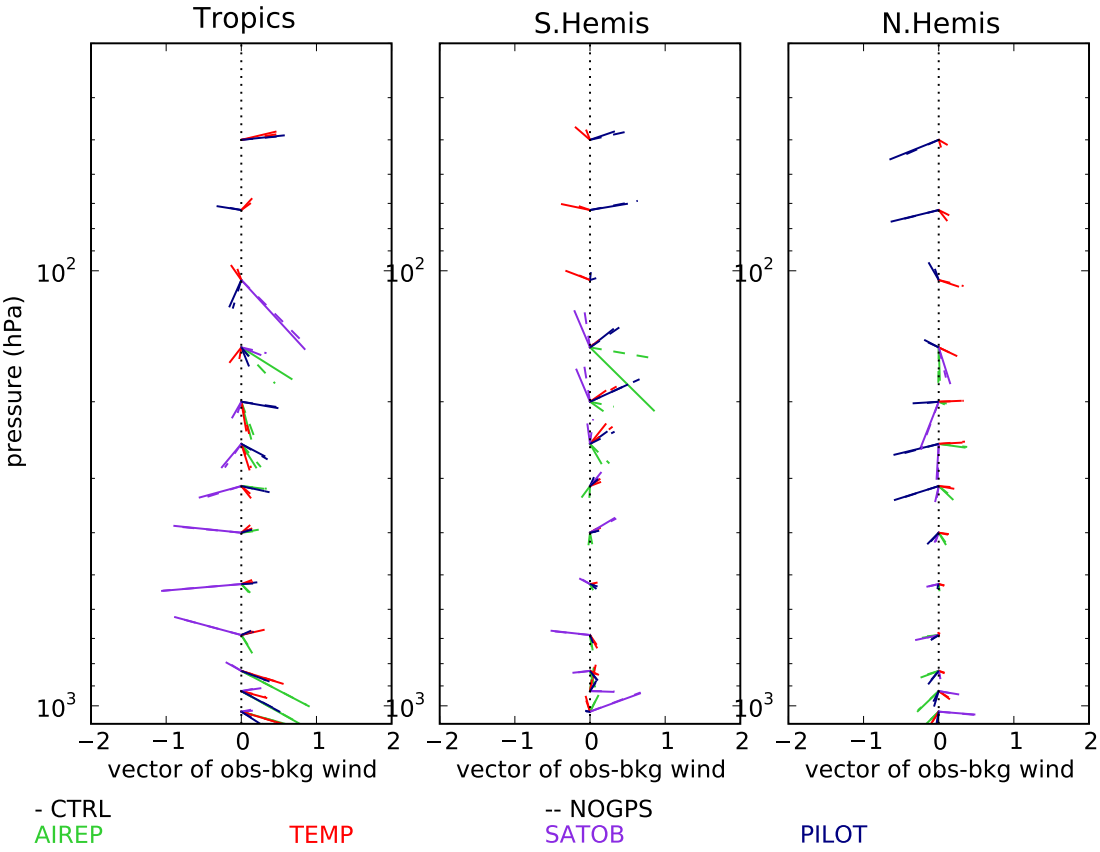

Figure 7.10: Mean wind vector (North direction is indicated by vertical axis, 1 m/s unit indicated on the horizontal axis) difference between observation and background

vations, shown in Figure 7.9. Similar results as for the zonal winds are observed with a small reduction in standard deviation difference when GPSRO data are assimilated. However, opposite results are obtained for the mean fit in the Southern Hemisphere, where the background with GPSRO data presents mean meridional zind differences that are shifted towards positive values between pressures 200–100 hPa, when validated against satellite winds and in situ wind observations. This suggests that the addition of GPSRO rotates the vector formed by the average zonal wind fit and average meridional wind fit. Figure 7.10 shows such vectors. In accordance with the previous discussion, the largest differences are observed in the Southern Hemisphere at pressure levels 200–100 hPa.

There are several possible explanations. First, the observations used for validation may present directional wind biases, and/or the model used in ERA-Interim could also have wind direction biases; then it is unclear whether the wind rotation caused by GPSRO data may be beneficial or detrimental. Second, the balance operator which acts to propagate the increments into the winds could be suboptimal so that the wind rotation could be an artefact of the assimilation. That conjecture seems to be contracticted by the fact that the addition of GPSRO data does reduce the wind fit to observations in a standard deviation sense.

8 Discussion

8.0.5 Stability of GPSRO data over time

The current re-analysis assimilated GPSRO data since 2001. Figure 5.1 shows that the mean fit between GPSRO data and the ERA-Interim background did not change much over time, except when additional data were introduced. This would seem to imply that the GPSRO data present a good stability over the time period covered here.

However, one obvious counter-remark would be to argue that, because the data were assimilated in the ERA-Interim system, any variations in the data would not show in the differences.

Consequently, to back our claim, we refer the reader to Figures 6.1 and 6.2. The radiosonde data used here were corrected for instrument changes by Haimberger (2007). They can thus be considered as a good reference for verifying the possible drift of the ERA-Interim system that could have been imposed by possible drifts in GPSRO data.

The time-series of mean differences between radiosonde temperatures and ERA-Interim do not exhibit any visible particular drift. The only visible differences are when additional GPSRO data are introduced. This is not a proof that GPSRO data may be free drift-free, but at least it shows that the effect of such drift, if any, is invisible on the ERA-Interim system when validated against radiosondes.

To demonstrate the climate stability of GPSRO data, besides a long collection of data, a proper set of proofs needs to be established to relate the atomic calibration of the GPS frequencies to the final (bending angle versus impact parameter) product. From the delay observable to its measurement by a receiver (with associated tracking software) and a retrieval step (including ionospheric correction), additional data (e.g. from a fiducial ground network, which can change over time) or assumptions (e.g., in the receiver loop tracking) are introduced. Some of these sources of possible discontinuities caused by changing practice can be reversed, for example when re-processing, using consistent methods, but others may not be possible (e.g. receiver acquisition loop design). Also, the current advanced wave processing methods usually applied in the lower troposphere (except so far for MetOp-A GRAS data) use both phase and amplitude data; it remains needs to be shown for example if a drift in the amplitude measurement could not propagate to a drift in the retrieval.

9 Considerations for future re-analysis

The ERA-Interim re-analysis has not assimilated all the GPSRO data that have been collected so far. Only the 'major' datasets made of CHAMP, COSMIC and now GRAS have been considered. The omitted GPSRO data include GPS/MET (launched in 1995), the Oersted satellite (launched in 1999), the Satelite de Aplicaciones Cientificas-C (SAC-C, launched in 2000, Hajj et al., 2002), and the Gravity Recovery and Climate Experiment (GRACE, launched in 2002, Beyerle et al., 2005). It remains to be determined how many profiles could be gathered from each of these experimental missions with today's progress in GPSRO data processing. We note that the Oersted data may present an interesting test of the GPSRO climate stability claim, since these data require different methods for processing (Larsen et al., 2005). In any case, it could be profitable in a future re-analysis to assimilate all these data, should they be available in the same format as currently distributed to NWP centers.

During the time period covered so far, the processing method employed by each data provider has not changed to the extent that the mean state observed by each GPSRO satellite has changed. As ERA-Interim continues to run in near-real-time and is fed with GPSRO data processed for NWP, this situation could change as data providers change their processing strategies. For example, one may expect that the implementation of an improved retrieval technique for MetOp-A GRAS data could affect the bias of GPSRO bending angles in the troposphere (although data below 8 km impact heights from that instrument are not used in ERA-Interim). Also the differences in bending angle between the several receivers and ERA-Interim were not always found to be perfectly zero, while they were found to be small for the various COSMIC receivers. It remains that it would probably be safer in a future re-analysis to use only data that were reprocessed using a consistent method for all receivers.

Two additional GRAS receivers are to be launched, onboard MetOp-B (2010) and MetOp-C (2014), with a goal to collect continuous measurements until the year 2020. We expect to assimilate these measurements should ERA-Interim still run at that time, and should the data quality be comparable to that of MetOp-A GRAS.

Another aspect to consider in future, longer re-analyses is the physical relationship between meteorological quantities and the atmospheric refractive index at radio frequencies. The work presented here assumed the formula of Smith and Weintraub (1953). Over the years new formulae have been devised to relate the atmospheric refractive index with pressure, temperature, humidity, and carbone dioxide concentration. The formula used in the present work thus ignored the CO_2 increase over the time period 2001–2009. More importantly, none of the new formulae make use of state-of-the-start laboratory measurements (Healy, 2009). It would thus be wise to revise these formulae for climate monitoring. The importance of non-ideal gas compressibility would also need to be better understood (Aparicio et al., 2009).

10 Conclusions and Future Work

The GPSRO bending angle data are assimilated in ERA-Interim since 2001. The daily usage rate of these data is the highest of all the meteorological observations. This suggests that these data are ready-to-use by today's re-analysis system in their current form.

The differences between GPSRO bending angle data and ERA-Interim contain a QBO signature in the tropics. Besides that signature, the mean differences appear stable over time. At the same time, differences between the ERA-Interim system and radiosondes are also found stable when the number of GPSRO data is stable. This suggests that the GPSRO bending angle used here are as stable as the radiosonde data use to compare with, or at least to the extent that we did not observe any visible drift between radiosonde observations and ERA-Interim nor between GPSRO observations and ERA-Interim.

Small differences are observed between bending angle data from the various satellites. The COSMIC data are all consistent with each other. The CHAMP data differ on average from the COSMIC data for the lowest levels; CHAMP features a larger negative bias than COSMIC, when compared to the ERA-Interim background. The GRAS data differ from COSMIC in the lower stratosphere; we observe a negative bias of 0.1% between GRAS bending angle observation and ERA-Interim background in that region, versus a virtually near-zero mean difference between COSMIC bending angle observation and ERA-Interim background.

We observe evidence of discontinuites in the ERA-Interim time-series when the number of GPSRO data is increased by a factor 10, with the introduction of COSMIC data end 2006. This has the effect of bringing ERA-Interim closer to the GPSRO and radiosonde temperature data especially at pressure levels 200–100 hPa, and further away from aircraft temperature data at the flight cruising altitude (around 200 hPa). The net effect of introducing many GPSRO (COSMIC) data end 2006 is to warm the lower stratosphere by 0.1–0.2 K and to cool the troposphere by less than 0.1 K. We also observe that the lower troposphere is drier over land after end 2006. These heuristic conclusions drawn from time-series observation are backed over land by radiosonde observations of temperature in all hemispheres and of humidity in the tropics.

The GPSRO data act to anchor the satellite radiance data bias corrected with a variational method (VarBC). The memory of the VarBC for some of these channels seems to be up to 2 months in an experiment where GPSRO data are withheld.

The GPSRO data are also found to act as a counter-balance against the warmly biased aircraft data in the recent years. However, a proper solution would be to correct the biased aircraft data (before assimilation, or in the assimilation, via a variational bias correction). This higlights the importance of being able to rely on GPSRO data to act as a reference for re-analysis, in addition to radiosonde temperatures in the upper troposphere and lower stratosphere in the recent years.

Finally, we also observe that adding GPSRO data improves the standard deviation fit of the ERA-Interim re-analysis to radiosonde temperature and wind observations. This indicates

that the variability represented in ERA-Interim is of better quality after end 2006 when large amounts of GPSRO data are assimilated.

More GPSRO missions than those whose data have been assimilated in the present work have collected GPSRO data. To benefit from these data in future re-analyses, efforts should be coordinated with GPSRO data processing centers to ensure consistent reprocessing and data access.

Acknowledgements

The GPSRO assimilated in ERA-Interim were provided by UCAR CDAAC, GFZ Potdsam, and Eumetsat. Funding to develop the GPSRO assimilation methodology was provided by the Eumetsat GRAS-Satellite Application Facility (GRAS-SAF).

References

Anderson E, Järvinen H. 1999. Variational quality control. Quart. J. Royal Meteorol. Soc. 125(554):697-722, DOI:10.1002/qj.49712555416

Anthes RA, Bernhardt PA, Chen Y, Cucurull L, Dymond KF, Ector D, Healy SB, Ho S-P, Hunt DC, Kuo Y-H, Liu H, Manning K, McCormick C, Meehan TK, Randel WJ, Rocken C, Schreiner WS, Sokolovskiy SV, Syndergaard S, Thompson DC, Trenberth KE, Wee T-K, Yen NL, Zeng Z. 2008. The COSMIC/FORMOSAT-3 mission: early results. Bull. Amer. Meteor. Soc. 89(3):313-333 DOI:10.1175/BAMS-89-3-313

Ao CO, Meehan TK, Hajj GA, Mannucci AJ, Beyerle G. 2003. Lower troposphere refractivity bias in GPS occultation retrievals. J. Geophys. Res. 108(D18):4577 DOI:10.1029/2002JD003216

Aparicio JM, Deblonde G, Garand L, Laroche S. 2009. Signature of the atmospheric compressibility factor in COSMIC, CHAMP, and GRACE radio occultation data. J. Geophys. Res. 114:D16114 DOI:10.1029/2008JD011156

Auligné T, McNally AP, Dee DP. 2007. Adaptive bias correction for satellite data in a numerical weather prediction system. Quart. J. Royal Meteorol. Soc. 133(624):631-642 DOI:10.1002/qj.56

Bengtsson L, Kanamitsu M, Kållberg P, Uppala S. 1982. FGGE 4-dimensional data assimilation at ECMWF. Bull. Amer. Meteor. Soc. 63:29-43

Beyerle G, Schmidt T, Michalak G, Heise S, Wickert J, Reigber C. 2005. GPS radio occultation with GRACE: Atmospheric profiling utilizing the zero difference technique. Geophys. Res. Lett. 32(13):L13806 DOI:10.1029/2005GL023109

Buontempo C, Jupp A, Rennie M. 2008. Operational NWP assimilation of GPS radio occultation data. Atmos. Sci. Lett. 9(3):129-133 DOI:10.1002/asl.173

Cucurull L, Derber JC, Treadon R, Purser R. 2007. Assimilation of Global Positioning System radio occultation observations into NCEP's Global Data Assimilation System. Mon. Wea. Rev. 35:3174-3193

Cheng CZF, Kuo YH, Anthes RA, Wu L. 2006. Satellite Constellation Monitors Global and Space Weather. Eos Trans. AGU 87(17) DOI:10.1029/2006EO170003

Dee DP. 2005. Bias and data assimilation. Quart. J. Royal Meteorol. Soc. 131(613):3323-3343 DOI:10.1256/qj.05.137

Dee D, Uppala SM. 2009. Variational bias correction of satellite radiance data in the ERA-Interim reanalysis. Quart. J. Royal Meteorol. Soc. in press

Derber J, Wu W-W. 1998. The use of TOVS cloud-cleared radiances in the NCEP SSI analysis system. Mon. Wea. Rev. 126(8):2287-2299

Foelsche U, Borsche M, Steiner AK, Gobiet A, Pirscher B, Kirchengast G, Wickert J, Schmidt T. 2007. Observing upper troposphere-lower stratosphere climate with radio occultation data from the CHAMP satellite. Climate Dyn. 31:49-65 DOI:10.1007/s00382-007-0337-7

Goody R, Anderson JG, North G. 1998. Testing climate models: An approach. Bull. Am. Meteorol. Soc. 79:2541?2549

Haimberger L. 2007. Homogenization of radiosonde temperature time series using innovation statistics. J. Clim. 20:1377-1403

Hajj GA, de la Torre Juarez M, Iijima BA, Kursinski ER, Mannucci AJ, Yunck TP. 2002. GPS radio occultations coming of age: Spacecraft launches add two new instruments for climate monitoring. Eos Trans. AGU 83(4):37

Healy SB. 2009. Refractivity coefficients used in the assimilation of GPS radio occultation measurements. GRAS-SAF Report 09. Available at: http://www.grassaf.org

Healy SB, Thépaut J-N. 2006. Assimilation experiments with CHAMP GPS radio occultation measurements. Quart. J. Royal Meteorol. Soc. 132(615):605-623 DOI:10.1256/qj.04.182

Hollingsworth A, Pfrang C. 2005. A preliminary survey of ERA-40 users developing applications of relevance to GEO (Group on Earth Observations). *European Centre for Medium-range Weather Forecasts Newsletter*. 104:5-9

Karbou F, Bormann N, Thépaut J-N. 2007. Towards the assimilation of satellite microwave observations over land: feasability studies using SSMI/S, AMSU-A and AMSU-B. NWP SAF Programme Research Report. Available from Meteo-France CNRM/GAME, 42 avenue Coriolis, 31057 Toulouse, France

Kuo, YH, Sokolovskiy S, Anthes R, Vandenberghe V. 2000. Assimilation of GPS radio occultation data for numerical weather prediction. Terr. Atmos. Oceanic Sci. 11:157-186

Kursinski ER, Hajj GA, Bertiger WI, Leroy SS, Meehan TK, Romans LJ, Schofield JT, McCleese DJ, Melbourne WG, Thornton CL, Yunck TP, Eyre JR, Nagatani RN. 1996. Initial results of radio occultation observations of Earth's atmosphere using the Global Positioning System. Science 271:1107-1110

Kursinski ER, Hajj GA, Schofield JT, Linfield RP, Hardy KR. 1997. Observing Earth's atmosphere with radio occultation measurements using the Global Positioning System. J. Geophys. Res. 102(D19):23429-23465

Larsen GB, Syndergaard S, Hoeg P, Soerensen MB. 2005. Single frequency processing of Oersted GPS radio occultation measurements. GPS Solut. 9(2):144-155

Leroy SS, Anderson JG, Dykema JA. 2006. Testing climate models using GPS radio occultation: A sensitivity analysis. J. Geophys. Res. 111:D17105 DOI:10.1029/2005JD006145

Logsdon T. 1995. *Understanding the NAVSTAR*, (2nd edn). Chapman and Hall

Luntama J-P, Kirchengast G, Borsche M, Foelsche U, Steiner A, Healy SB, von Engeln A, O'Clerigh E, Marquardt C. 2008. Prospects of the EPS GRAS mission for operational atmospheric applications. Bull. Amer. Meteor. Soc. 89(12):1863-1875 DOI:10.1175/2008BAMS2399.1

Ploshay J, Stern W, Miyakoda K. 1992. FGGE Reanalysis at GFDL. Mon. Wea. Rev. 120(9):2083-2108

Poli P, Healy SB, Rabier F, Pailleux, J. 2008. Preliminary assessment of the scalability of GPS radio occultations impact in numerical weather prediction. Geophys. Res. Lett. 35:L23811 DOI:10.1029/2008GL035873

Poli P, Moll P, Puech D, Rabier F, Healy SB. 2009. Quality control, error analysis, and impact assessment of FORMOSAT-3/COSMIC in numerical weather prediction. Terr. Atmos. Ocean. 20(1):101-113 DOI:10.3319/TAO.2008.01.21.02(F3C)

Ringer MA, Healy SB. 2008. Monitoring twenty-first century climate using GPS radio occultation bending angles. Geophys. Res. Lett. 35:L05708 DOI:10.1029/2007GL032462

Schmidt T, Wickert J, Beyerle G, Reigber C. 2004. Tropical tropopause parameters derived from GPS radio occultation measurements with CHAMP. J. Geophys. Res. 109:D13105 DOI:10.1029/2004JD004566

Smith EK, Weintraub S. 1953. The constants in the equation for the atmospheric refractive index at radio frequencies. Proc. IRE 41:1035-1037

Steiner AK, Kirchengast G. 2005. Error analysis for GNSS radio occultation data based on ensembles of profiles from end-to-end simulations. J. Geophys. Res. 110:D15307 DOI:10.1029/2004JD005251

Steiner AK, Kirchengast G, Lackner BC, Pirscher B, Borsche M, Foelsche U. 2009. Atmospheric temperature change detection with GPS radio occultation 1995 to 2008. Geophys. Res. Lett. 36:L18702 DOI:10.1029/2009GL039777

Syndergaard S. 1999. Retrieval analysis and methodologies in atmospheric limb sounding using the GNSS radio occultation technique, Dissertation, Niel Bohr Institute for Astronomy, Physics and Geophysics, Faculty of Science, University of Copenhagen, Denmark

Uppala SM, Kållberg PW, Simmons AJ, Andrae U, Da Costa Bechtold V, Fiorino M, Gibson JK, Haseler J, Hernandez A, Kelly GA, Li X, Onogi K, Saarinen S, Sokka N, Allan RP, Andersson E, Arpe K, Balmaseda MA, Beljaars ACM, Van De Berg L, Bidlot J, Bormann N, Caires S, Chevallier F, Dethof A, Dragosavac M, Fisher M, Fuentes M, Hagemann S, Hólm E, Hoskins BJ, Isaksen L, Janssen PAEM, Jenne R, Mcnally AP, Mahfouf J-F, Morcrette J-J, Rayner NA, Saunders RW, Simon P, Sterl A, Trenberth KE, Untch A, Vasiljevic D, Viterbo P, Woollen J. 2005. The ERA-40 re-analysis. Quart. J. Royal Meteorol. Soc. 131(612):2961-3012 DOI:10.1256/qj.04.176

Uppala SM, Dee D, Kobayashi S, Berrisford P, Simmons A. 2008. Towards a climate data assimilation system: status update of ERA-Interim. *European Centre for Medium-range Weather Forecasts Newsletter*. 115:12-18

Ware R, Exner M, Feng D, Gorbunov M, Hardy K, Herman B, Kuo Y, Meehan T, Melbourne W, Rocken C, Schreiner W, Sokolovskiy S, Soltheim F, Zou X, Anthes R, Businger S, Trenberth K. 1996. GPS Sounding of the atmosphere from low Earth orbit: preliminary results. Bull. Amer. Meteor. Soc. 77 (1): 19-40

Wickert J, Reigber C, Beyerle G, König R, Marquardt C, Schmidt T, Grunwaldt L, Galas R, Meehan TK, Melbourne WG, Hocke K. 2001. Atmosphere sounding by GPS radio occultation: first results from CHAMP. Geophys. Res. Lett. 28(17):3263-3266

GRAS SAF Reports

SAF/GRAS/METO/REP/GSR/001	Mono-dimensional thinning for GPS Radio Occulation
SAF/GRAS/METO/REP/GSR/002	Geodesy calculations in ROPP
SAF/GRAS/METO/REP/GSR/003	ROPP minimiser - minROPP
SAF/GRAS/METO/REP/GSR/004	Error function calculation in ROPP
SAF/GRAS/METO/REP/GSR/005	Refractivity calculations in ROPP
SAF/GRAS/METO/REP/GSR/006	Levenberg-Marquardt minimisation in ROPP
SAF/GRAS/METO/REP/GSR/007	Abel integral calculations in ROPP
SAF/GRAS/METO/REP/GSR/008	ROPP thinner algorithm
SAF/GRAS/METO/REP/GSR/009	Refractivity coefficients used in the assimilation of GPS radio occultation measurements
SAF/GRAS/METO/REP/GSR/010	Latitudinal Binning and Area-Weighted Averaging of Irregularly Distributed Radio Occultation Data
SAF/GRAS/METO/REP/GSR/011	ROPP 1dVar validation
SAF/GRAS/METO/REP/GSR/012	Assimilation of Global Positioning System Radio Occultation Data in the ECMWF ERA-Interim Re-analysis
SAF/GRAS/METO/REP/GSR/013	ROPP PP validation

GRAS SAF Reports are accessible via the GRAS SAF website http://www.grassaf.org.